AN ANALYTIC AND EXPERIMENTAL STUDY OF THE EFFECTS OF SPLITTER PLATE POSITION ON THE TRAILING EDGE MODIFICATIONS OF A CAMBERED CIRCULATION CONTROLLED ELLIPTICAL AIRFOIL

Richard K. deJonckheere

Air Force Institute of Technology
Wright-Patterson Air Force Base, Ohio

December 1975

DISCLAIMER NOTICE

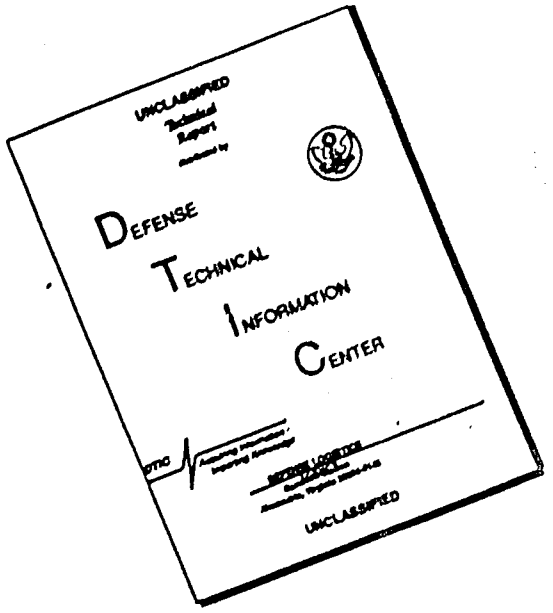

THIS DOCUMENT IS BEST QUALITY AVAILABLE. THE COPY FURNISHED TO DTIC CONTAINED A SIGNIFICANT NUMBER OF PAGES WHICH DO NOT REPRODUCE LEGIBLY.

KEEP UP TO DATE

Between the time you ordered this report—which is only one of the hundreds of thousands in the NTIS information collection available to you—and the time you are reading this message, several *new* reports relevant to your interests probably have entered the collection.

Subscribe to the **Weekly Government Abstracts** series that will bring you summaries of new reports *as soon as they are received by NTIS* from the originators of the research. The WGA's are an NTIS weekly newsletter service covering the most recent research findings in 25 areas of industrial, technological, and sociological interest—invaluable information for executives and professionals who must keep up to date.

The executive and professional information service provided by NTIS in the **Weekly Government Abstracts** newsletters will give you thorough and comprehensive coverage of government-conducted or sponsored research activities. And you'll get this important information within two weeks of the time it's released by originating agencies.

WGA newsletters are computer produced and electronically photocomposed to slash the time gap between the release of a report and its availability. You can learn about technical innovations immediately—and use them in the most meaningful and productive ways possible for your organization. Please request NTIS-PR-205/PCW for more information.

The weekly newsletter series will keep you current. But *learn what you have missed in the past* by ordering a computer **NTISearch** of all the research reports in your area of interest, dating as far back as 1964, if you wish. Please request NTIS-PR-186/PCN for more information.

WRITE: Managing Editor
5285 Port Royal Road
Springfield, VA 22161

Keep Up To Date With SRIM

SRIM (Selected Research in Microfiche) provides you with regular, automatic distribution of the complete texts of NTIS research reports *only* in the subject areas you select. SRIM covers almost all Government research reports by subject area and/or the originating Federal or local government agency. You may subscribe by any category or subcategory of our WGA **(Weekly Government Abstracts)** or **Government Reports Announcements and Index** categories, or to the reports issued by a particular agency such as the Department of Defense, Federal Energy Administration, or Environmental Protection Agency. Other options that will give you greater selectivity are available on request.

The cost of SRIM service is only 45¢ domestic (60¢ foreign) for each complete microfiched report. Your SRIM service begins as soon as your order is received and processed and you will receive biweekly shipments thereafter. If you wish, your service will be backdated to furnish you microfiche of reports issued earlier.

Because of contractual arrangements with several Special Technology Groups, not all NTIS reports are distributed in the SRIM program. You will receive a notice in your microfiche shipments identifying the exceptionally priced reports not available through SRIM.

A deposit account with NTIS is required before this service can be initiated. If you have specific questions concerning this service, please call (703) 451-1558, or write NTIS, attention SRIM Product Manager.

This information product distributed by

NTIS U.S. DEPARTMENT OF COMMERCE
National Technical Information Service
5285 Port Royal Road
Springfield, Virginia 22161

UNCLASSIFIED

SECURITY CLASSIFICATION OF THIS PAGE (When Data Entered)

REPORT DOCUMENTATION PAGE		READ INSTRUCTIONS BEFORE COMPLETING FORM
1. REPORT NUMBER GAE/AE/75D-12	2. GOVT ACCESSION NO.	3. RECIPIENT'S CATALOG NUMBER AD A022 3354
4. TITLE (and Subtitle) AN ANALYTIC AND EXPERIMENTAL STUDY OF THE EFFECTS OF SPLITTER PLATE POSITION ON THE TRAILING EDGE MODIFICATIONS OF A CAMBERED CIRCULATION CONTROLLED ELLIPTICAL AIRFOIL		5. TYPE OF REPORT & PERIOD COVERED MS Thesis 6. PERFORMING ORG. REPORT NUMBER
7. AUTHOR(s) Richard K. de Jonckheere 2Lt USAF		8. CONTRACT OR GRANT NUMBER(s)
9. PERFORMING ORGANIZATION NAME AND ADDRESS Air Force Institute of Technology (AFIT-EN) Wright-Patterson AFB, Ohio 45433		10. PROGRAM ELEMENT, PROJECT, TASK AREA & WORK UNIT NUMBERS
11. CONTROLLING OFFICE NAME AND ADDRESS Aeronautical Systems Division (ASD/XRHD) Wright-Patterson AFB, Ohio 45433		12. REPORT DATE December, 1975 13. NUMBER OF PAGES 84
14. MONITORING AGENCY NAME & ADDRESS(if different from Controlling Office)		15. SECURITY CLASS. (of this report) Unclassified 15a. DECLASSIFICATION DOWNGRADING SCHEDULE

16. DISTRIBUTION STATEMENT (of this Report)

Approved for public release; distribution unlimited

17. DISTRIBUTION STATEMENT (of the abstract entered in Block 20, if different from Report)

SUBJECT to C...

18. SUPPLEMENTARY NOTES

Approved for public release; IAW AFR 190-17

JERRY C. HIX, Captain, USAF
Director of Information

19. KEY WORDS (Continue on reverse side if necessary and identify by block number)

Airfoil Testing
Boundary Layer Control
Blowing Slot
Circulation Control
High Lift Devices
Potential Flow Theory

20. ABSTRACT (Continue on reverse side if necessary and identify by block number)

See reverse side.

DD FORM 1 JAN 73 1473 EDITION OF 1 NOV 65 IS OBSOLETE

UNCLASSIFIED

SECURITY CLASSIFICATION OF THIS PAGE (When Data Entered)

Block #20

Wind tunnel tests were conducted to determine the effects of splitter plate position on trailing edge modifications of a circulation controlled airfoil. Analytic studies were conducted to determine the feasibility of using a potential flow computer program to predict the results of the wind tunnel tests. The airfoil model was elliptical in shape, 20 percent thick, and had five percent camber. It employed a blowing slot for circulation control and a splitter plate for reduction in mixing losses. Modifications included slot positions on the upper surface of 96 and 97 percent chord, slot angles of +5 and -33 degrees, circular and elliptic aft contours, and splitter plate positions on the lower surface of 99 and 95.3 percent chord. Tests were conducted at a Reynolds number of 7.4×10^5 and blowing momentum coefficients of zero and 0.03.

The lift-to-drag ratio of the airfoil was increased by use of a splitter plate over a clean configuration and was maximized with the splitter plate at the 99 percent chord position. These results held true for variations in slot position, angle, aft contour, and blowing rate.

The potential flow computer program was capable of achieving lift coefficients obtained in wind tunnel tests. However, due to an inviscid flow assumption, the program was not feasible for prediction purposes.

1 a

GAE/AE/75D-12

AN ANALYTIC AND EXPERIMENTAL STUDY OF THE EFFECTS OF SPLITTER PLATE POSITION ON THE TRAILING EDGE MODIFICATIONS OF A CAMBERED CIRCULATION CONTROLLED ELLIPTICAL AIRFOIL

THESIS

GAE/AE/75D-12 Richard K. deJonckheere
2d Lt USAF

Approved for public release; distribution unlimited.

A

GAE/AE/75D-12

AN ANALYTIC AND EXPERIMENTAL STUDY OF THE EFFECTS OF SPLITTER PLATE POSITION ON THE TRAILING EDGE MODIFICATIONS OF A CAMBERED CIRCULATION CONTROLLED ELLIPTICAL AIRFOIL

THESIS

Presented to the Faculty of the School of Engineering

of the Air Force Institute of Technology

Air University

in Partial Fulfillment of the

Requirements for the Degree of

Master of Science

by

Richard K. de Jonckheere, B.S.

2d Lt USAF

Graduate Aerospace-Mechanical Engineering

December 1975

Preface

This study was an experimental and analytic investigation of the effect of a splitter plate on the trailing edge modifications of a cambered, circulation controlled, elliptical airfoil. It is hoped that the results of this study stimulate more research towards predicting and improving the lift-to-drag ratio of circulation controlled, high-lift devices.

I would like to express my appreciation to Dr. Milton E. Franke, my advisor, Mr. James Snyder, ASD/XRHD, and Majors Roger Crawford and Carl Stolberg for their assistance throughout the project. Special thanks go to Mr. Millard Wolfe and the AFIT workshop staff for their valuable assistance in design and ability in construction of the modified endpieces and associated equipment. Thanks also go to Mr. Wales S. Whitt for his assistance during wind tunnel set-up and testing.

Further gratitude is expressed to Mr. Julius Becsey, AFAPL, who wrote the data reduction computer programs and made his equipment available for data reduction purposes. Appreciation is also expressed to Mr. George Lorraine, of Tech Photo, and his staff for excellent photographic support of the project. Finally, many thanks go to 2/Lt Vayl S. Oxford for his patience and support through this endeavor.

Richard K. deJonckheere

Contents

Contents

List of Figures

List of Figures

List of Figures

List of Figures

List of Tables

List of Symbols

English Letters

A	Potential flow program variable
c	Chord length of airfoil model, ft
C_d	Section profile drag coefficient
C_{d_t}	Section total drag coefficient
C_l	Section lift coefficient
C_n	Section normal force coefficient
C_p	Pressure coefficient
C_{p_l}	Pressure coefficient on airfoil lower surface
C_{p_u}	Pressure coefficient on airfoil upper surface
C_μ	Blowing momentum coefficient
C_{V_N}	Coefficients of program surface normal velocity
h	Wind tunnel test section height, ft
L/D	Lift-to-drag ratio
$\dot{m}$	Mass flow rate per unit span, $lb_m/sec/ft$
P_l	Local static pressure, psfg
P_o	Free stream static pressure, psfg
q	Local dynamic pressure, psfg
q_o	Free stream dynamic pressure, psfg
R_e	Reynolds number, $\frac{\rho V c}{\mu}$
U_o	Program free stream velocity
u	Program chordwise velocity component

v	Program vertical velocity component
V_T	Program surface tangential velocity
V_N	Program surface normal velocity
V_j	Slot velocity in tests, ft/sec
V_o	Free stream velocity in tests, ft/sec
x	Chordwise ordinate, ft
x_c	Program chordwise ordinate of control points, in.
x_v	Program chordwise ordinate of vortex points, in.
y	Vertical ordinate, ft
y_c	Program vertical ordinate of control points, in.
y_v	Program vertical ordinate of vortex points, in.

Greek Letters

α	Geometric angle of attack, degrees
β	Splitter plate deflection, degrees
Γ	Program vortex strength
ϕ_v	Program potential function of vortex
θ	Program slope of surface, radians

Abstract

Wind tunnel tests were conducted to determine the effects of splitter plate position on trailing edge modifications of a circulation controlled airfoil. Analytic studies were also conducted to determine the feasibility of using a potential flow computer program to predict the results of the wind tunnel tests. The airfoil model was elliptical in shape, 20 percent thick, and had five percent camber. It employed a blowing slot for circulation control and a splitter plate for reduction in mixing losses. Modifications included slot positions on the upper surface of 96 and 97 percent chord, slot angles of +5 and -33 degrees, circular and elliptical aft contours, and splitter plate positions on the lower surface of 99 and 95.3 percent chord. Tests were conducted at a Reynolds number of 7.4×10^5 and blowing momentum coefficients of zero and 0.03.

The lift-to-drag ratio of the airfoil was increased with the use of a splitter plate over a clean configuration and was maximized with the splitter plate at the 99 percent chord position. These results held true for the variations in slot position, slot angle, aft contour, and blowing rate.

The potential flow computer program was capable of matching lift coefficients obtained in wind tunnel tests. However, due to an inviscid flow assumption, the program was not feasible for prediction purposes because it did not model the flow accurately.

GAE/AE/75D-12

AN ANALYTIC AND EXPERIMENTAL STUDY OF THE EFFECTS OF SPLITTER PLATE POSITION ON THE TRAILING EDGE MODIFICATIONS OF A CAMBERED CIRCULATION CONTROLLED ELLIPTICAL AIRFOIL

I. Introduction

During the past several years a great interest has developed in aeronautical structures that improve low-speed, high-lift capabilities. The motivation for this interest is the desire that aircraft land and takeoff in shorter distances than normal. Short-takeoff-and-landing aircraft (STOL) have this as a requirement for their missions, as they must enter and leave areas normally inaccessible to aircraft. Reconnaissance and forward control aircraft have need of the ability to loiter around target areas, therefore requiring a low-speed, high-lift capability. Supersonic fighters, primarily designed for high speed flight, normally do not perform well at the lower speeds and need more lift during landing and takeoff. Thus, high-lift structures, or wings, that perform well at lower speeds would greatly enhance these missions.

Poor performance at lower speeds, where higher lift is needed, is due to separation of the flow around the wing. This is a result of

the fact that the flow loses energy near the trailing edge of the wing at high angles of attack and can no longer remain attached to the surface. This separation of flow actually decreases the lift of the wing, and thus of the whole aircraft.

Previous Work

Through studies done in the past, it is known that the flow around a body can be re-energized to help it remain attached to the surface at high angles of attack. The ways of re-energizing this flow before it separates are called circulation control methods, and include suction, blowing, and cooling of the surface. The blowing method is the primary concern of this present study. Blowing, or injecting air into the already existing flow, adds energy to the flow by increasing its velocity and helps prevent it from becoming detached from the surface.

This method of circulation control was emphasized in previous experimental studies by many researchers. Kind and Maull investigated a low-speed, circulation-controlled, elliptic airfoil with blowing near the trailing edge, and achieved fairly high coefficients of lift (Ref 2). Englar (Ref 1), with another elliptic airfoil, achieved higher lift coefficients than Kind and Maull. Williams and Howe, with a slightly thicker and more cambered airfoil than Englar, achieved even higher coefficients of lift (Ref 6). Stevenson (Ref 5) and Rhynard (Ref 4), at the Air Force Institute of Technology (AFIT),

made similar studies but they also made use of a splitter plate. The splitter plate was mounted on the lower surface near the trailing edge, and it spanned the model. It was designed to reduce mixing losses near the trailing edge and resulted in higher lift coefficients and lower drag coefficients. Thus, there is much known about circulation control, but still remains a large area to investigate, even with the blowing method.

Present Study

The purpose of this study was to further the investigation of the circulation control method of blowing air onto the trailing edge. The principal goal was to study the effec. of splitter plate positions, or lower surface configurations, on various methods of flow acceleration and trailing edge flow treatment. An analytic study was also conducted through the use of potential flow theory and computational methods in an attempt to predict the re ults of these variations.

Scope

This study was conducted in two phases. The first phase consisted of researching and formulating feasible model modifications that would produce variations in flow acceleration and trailing edge flow treatment. Variations in flow acceleration were made by changing the blowing slot location and angle. Flow treatment variations

were made by changing the aft contour. The splitter plate positions to be used in testing were then determined. This phase also included the development of the potential flow model that would be used to predict results of the wind tunnel testing.

The second phase of the study was the testing of the model with modifications in the AFIT Five-Foot Wind Tunnel. It included the manipulation of the potential flow computer program to predict the results achieved in the actual testing. The wind tunnel testing was conducted with modified endpieces that had only one variation each, from the original, of the slot position, the slot angle, and aft contour. The configuration on the trailing edge lower surface was also varied for each endpiece from clean to a splitter plate in the 99 percent chord position, and to a splitter plate in the 95.3 percent chord position. The tests were conducted through a range of angles of attack from -6 to +6 degrees, at blowing momentum coefficients of zero and 0.03, and at a Reynolds number of 7.4×10^5. The variations in the endpieces, the lower surface, the angles of attack, and momentum coefficients were incorporated into the potential flow computer program. The resulting coefficients of lift were then compared to the actual wind tunnel data to determine if the method was suitable for prediction purposes.

II. Preliminary Investigation

The purpose of the preliminary investigation was to determine what modifications were to be made on the airfoil and what lower surface configurations were to be used in the wind tunnel testing. Previous studies were investigated and it was determined that variations of three characteristics of the trailing edge of the model should be considered. These characteristics were the blowing slot position, its angle, and the aft contour.

The slot location is an important factor in improving lift-to-drag ratios. The further forward the slot is located, the larger the momentum coefficient needed to effectively turn the flow around the trailing edge. The further aft the slot is located, the larger the momentum coefficient needed to prevent separation of the flow at high angles of attack. Thus, a variation in the slot position was considered and two positions were chosen.

The slot angle is also an important factor in improving lift-to-drag ratios. The more tangential the air is injected into the surface flow, the more effectively it re-energizes that flow and helps it remain attached to the surface around the trailing edge. Therefore, a change in the slot angle was also considered and two angles were used.

The effect of the aft contour had been investigated previously in the studies of Kind (Ref 2), Williams (Ref 6), and Englar (Ref 1). They found that the turning of the flow was more effective with a more circular trailing edge. However, this more effective turning also produced greater losses when the upper and lower surface flows mixed. These results led to more lift but increased drag. Thus, an optimum combination of circular and elliptic trailing edge contours was recommended. Based on this, two contours were chosen.

The last area studied was the lower surface configuration. In the investigations of Rhynard (Ref 4) and Stevenson (Ref 5), a splitter plate was used on the lower surface. The splitter plate was designed to reduce the losses due to mixing of the lower and upper surface air flows as they neared the trailing edge. Stevenson determined the necessity of such a splitter plate and Rhynard attempted to optimize the position on the lower surface and the angle of the splitter plate. Based on Rhynard's results, three configurations were used in this study.

As a result of this preliminary investigation, four endpieces, to be mounted on the airfoil, were designed and constructed for tests in the AFIT Five-Foot Wind Tunnel. The endpieces differed from each other by a single variation in one of the characteristics. Each endpiece also allowed for the use of a splitter plate in various positions.

III. Description of Apparatus

Wind Tunnel

Wind tunnel tests were conducted in the AFIT Five-Foot Wind Tunnel. The tunnel, an open return induction type, has a maximum flow speed of 250 miles per hour. Two large plyboard side panels were installed in the five-foot diameter test section to simulate a two-dimensional test section 60 in. high and 30 in. wide. The trailing edges of the side panels were hinged flaps and attached to servos to control the angle. Four pitot-static tubes were installed at the entrance of the test section on the bottom, top, right and left sides, and measured the local dynamic pressure q. To insure that these four local q's remained essentially equal, the hinged flaps of the side panels were adjusted with the servos. As a result, a more uniform flow was maintained in the test section.

Eight static ports evenly spaced around the circumference of the tunnel measured the static pressure at the entrance to the test section. The difference between the static pressure and the atmospheric pressure was recorded on a micro-manometer filled with water and designated the tunnel head or "tunnel q."

Airfoil

The airfoil model was a 20 percent thick, five percent cambered, elliptical airfoil. The model had a span of 2.17 feet and

a chord of 1.67 feet. A sketch of the cross section of the airfoil is shown in Fig. 1.

The airfoil was equipped with 48 surface static pressure taps used to measure the pressure distribution around the airfoil. Forty-four of the taps were located along center span and concentrated toward the leading and trailing edges where greater pressure changes occur. Four taps were located off the center of the span near the blowing slot to check the spanwise uniformity of the flow. Three pitot tubes were located inside the plenum chamber of the airfoil to measure plenum total pressure and to check the spanwise uniformity of the flow exiting the slot.

Large circular aluminum sideplates were fitted to each side of the airfoil model. They were $\frac{3}{16}$ of an inch thick and beveled to 30 degrees at the edges. The purpose of these sideplates was to strip off the boundary layer that formed on the plyboard side panels and to aid in making the flow more nearly two-dimensional. The left sideplate also served as an attachment point for cables from the angle-of-attack drive mechanism. The cables were attached to the front and rear edges of the sideplate and were run through the tunnel floor to a motor driven gear box. The gear box, in turn, was connected to a revolution counter calibrated to an accuracy of three minutes of arc.

The blowing or secondary air system in the model consisted of a fiberglass plenum chamber and annealed copper pipe. Both chamber and pipe extended the span of the model. A cross section of

the plenum chamber and inlet pipe also appear in Fig. 1. Secondary air entered through the left side of the model into the inlet pipe. From the pipe, the airflow entered the plenum chamber, designed as a diverging-converging nozzle. The minimum area of the converging portion of the chamber served as the blowing slot from which air exited onto the trailing edge surface.

Four endpieces, constructed to be mounted on the airfoil, were tested. The endpieces were designated as Endpieces A, B, C, and D. The different endpieces appear in Figures 2 and 3 and are listed in Table I.

Table I

The Four Endpieces Used in the Wind Tunnel Tests

Endpiece	Slot Position	Slot Angle	Contour
A	96% chord	+ 5 degrees	elliptical
B	96% chord	- 33 degrees	elliptical
C	96% chord	+ 5 degrees	circular
D	97% chord	+ 5 degrees	elliptical

Endpiece A was similar in construction to the trailing edge configuration used by Stevenson and Rhynard. The slot angle on Endpiece B was constructed to be more nearly tangential to the surface. The circular contour on Endpiece C had a radius of 0.95 inches. The slots in the four endpieces were located on the upper surface and

extended across the span of the endpieces. Each slot was 0.020 inches high, fixed at a height to chord ratio of 0.001, and uniform to $\pm$ 0.0015 inches along the span.

Three configurations of splitter plates were tested on each endpiece. They were designated as No Splitter Plate, Aft Splitter Plate, and Forward Splitter Plate. The splitter plate used had a chord length of 1.5 inches. The No Splitter Plate configuration had no splitter plate on the lower surface and meant that the airfoil was clean. The Aft Splitter Plate configuration had the splitter plate at the 99 percent chord position and at an angle of -45 degrees from the chord line. The splitter plate in the Forward Splitter Plate configuration was located at the 95.3 percent chord position and at angle of -60 degrees from the chord line. The latter two configurations were chosen because they were found by Rhynard (Ref 4) to be optimum configurations. These configurations appear in Figures 2 and 3.

Flowmeter

The flowmeter used to measure the mass flow rate was a one inch diameter tube venturi with a throat diameter of 0.50 inches. It was calibrated against a National Bureau of Standards venturi. The temperature of the air flowing through the venturi was measured by a copper-constantan thermocouple inserted just upstream of the throat.

Wake Survey Rake

A total head wake survey rake, designed to measure the momentum deficit of the airfoil wake, was positioned 37 inches, or 1.85 chord lengths, behind the airfoil. The rake had 96 total head tubes and two static tubes. The tubes were 0.0625 inches in outside diameter and spaced 0.25 inches apart. The airfoil section of the rake spanned the tunnel from top to bottom and was adjustable within certain limitations.

Manometers

Two manometer banks were used to measure the pressure distributions on the airfoil surface and the wake survey rake. A 96 inch, 100-tube bank of vertical manometers containing alcohol was connected to the pressure taps on the airfoil. A 30 inch, 100-tube manometer bank containing red oil was connected to the wake survey rake. The bank was inclined 60 degrees from the vertical so that pressure changes on the rake could be read more accurately.

Two 60 inch vertical mercury manometers were used with the flowmeter to measure the secondary air flow rate. Finally, a mercury manometer bank was connected to the plenum chamber pitot tubes to measure the total pressure in the chamber.

Pitot Tube

A small pitot tube was constructed to measure the slot spanwise total pressure distribution. The outside diameter was 0.018 inches so that the pitot tube was able to fit into the slot.

IV. Experimental Procedure

The same general test procedure was ued on each of the four model and endpiece configurations. Once the endpiece was put on the model it was checked for leaks and uniformity of spanwise flow. The tunnel speed was then brought up to 1.25 inches of H_2O, corresponding to a nominal 74 feet per second. The geometric angle of attack was varied from -6 to +6 degrees in increments of two degrees. At each angle of attack the two manometer banks were photographed and data recorded from the flowmeter and plenum chamber manometers. After the angle of attack sequence was completed, the secondary air system was started and blowing rate adjusted to 22 inches of mercury on the flowmeter manometer. This corresponded to a blowing momentum coefficient, C_μ, of approximately 0.03. The angle of attack sequence was then repeated for this blowing rate. The tunnel speed was reduced to zero and the splitter plate was mounted in the aft position. The complete process was repeated for this configuration and then, after the splitter plate was remounted in the forward position, was repeated again for that configuration. Test runs were repeated for Endpieces A and B as a check for accuracy.

V. Data Reduction

Data obtained in the wind tunnel tests were reduced to three primary parameters. The parameters were the blowing momentum coefficient, the section lift coefficient, and the section total drag coefficient. These parameters were then used to calculate the lift-to-drag ratios of the various model and endpiece configurations.

Momentum Coefficient

The momentum coefficient is a measure of the amount of blowing applied to a circulation controlled airfoil. It is defined as

$$C_\mu = \frac{\dot{m} V_j}{q_o c} \tag{1}$$

where $\dot{m}$ is the mass flow rate of air per unit span, V_j is the velocity of the air jet at the slot, q_o is the free stream dynamic pressure, and c is the chord length of the airfoil (Ref 5:16).

Section Lift Coefficient

The section lift coefficient was calculated by the equation:

$$C_l = C_n \cos \alpha \tag{2}$$

where α is the geometric angle of attack and C_n is the section normal force coefficient. C_n was calculated by numerical integration of the pressure coefficients around the airfoil. The pressure coefficient is

defined as

$$C_p = \frac{P_l - P_o}{q_o} \tag{3}$$

Integration was accomplished according to the equation:

$$C_n = \int_o^1 \left(C_{p_l} - C_{p_u} \right) \, d \left(\frac{x}{c} \right) \tag{4}$$

where C_{p_l} and C_{p_u} are pressure coefficients on the lower and upper surfaces, respectively, and $\frac{x}{c}$ is the distance on the chord line (Ref 5:17). This was performed on the Hewlett-Packard 9100A Calculator with 9107A Digitizer.

Section Total Drag Coefficient

The section total drag coefficient takes into account the section profile drag coefficient, an intake penalty coefficient, and the blowing momentum coefficient. The section total drag coefficient is determined by the equation:

$$C_{d_t} = C_d + C_\mu + \frac{\dot{m} V_o}{q_o c} \tag{5}$$

The section profile drag coefficient was calculated from the momentum method and compares the momentum ahead of the model with the momentum behind the model. It is defined as

$$C_d = \frac{2}{c} \int_o^h \left(\sqrt{\frac{q}{q_o}} - \frac{q}{q_o} \right) dy \tag{6}$$

where q and q_o are the wake and free stream dynamic pressures, respectively, and dy is the incremental distance between tubes on the rake (Ref 5:18). The integration was performed by the trapezoidal rule of integration on the Hewlett-Packard 9100A Calculator with 9107A Digitizer. An intake penalty coefficient, from Englar (Ref 1:10), is applied because there is an increase in drag associated with the production of the blowing air from the free stream through the system to the slot. The momentum coefficient term, C_μ, is added because some of the momentum originated inside the model and this momentum actually decreased the momentum deficit that represents the drag. The two additional terms were included in calculation of the section total drag coefficient in order to allow for comparison to unblown airfoils.

Lift-to-Drag Ratio

The lift-to-drag ratio was calculated by taking the ratio of the section lift coefficient to the section total drag coefficient. The equation is

$$\frac{L}{D} = \frac{C_l}{C_{d_t}} \tag{7}$$

Wind Tunnel Corrections

Correction factors were applied to the wind tunnel data as the wind tunnel has solid boundaries and did not represent the free

stream atmosphere accurately. The presence of the model in the test section caused the free stream velocity to increase as it flowed over the model and the presence of the floor and ceiling prevented normal curvature of the flow. To account for these characteristics, streamline curvature corrections were applied to C_l while wake and solid blocking corrections were applied to C_l, C_d, q_o, and R_e. A wake survey rake correction factor was checked to apply to the pressure readings but it was negligible.

VI. Analytic Study

The analytic study consisted of the development and manipulation of a potential flow computer program. Its purpose was to predict results obtained in wind tunnel testing of the four endpieces, with various splitter plate configurations. It was based on potential theory and assumed inviscid, incompressible flow.

Development

The airfoil surface was segmented into 60 panels and panel size became smaller at the leading and trailing edges so as to weight these more sensitive areas. A vortex was located on each panel at the $\frac{1}{4}$ chord point and a control point was located at the $\frac{3}{4}$ chord point. This paneling scheme modeled the airfoil configuration without a splitter plate. To model the airfoil with a splitter plate, two additional panels were affixed to the lower surface in the appropriate position near the trailing edge. The three configurations of no splitter plate, aft splitter plate, and forward splitter plate are represented in Fig. 4. The splitter plates in the program are not the same size as in the tests because it was found that the thickness and length do not have a significant effect in potential flow theory.

The next step in the development was to solve for the particular vortex strengths, with the boundary condition that normal velocity through the surface was zero. From these, the lift coefficients

were calculated. The potential function for a vortex is given by the equation:

$$\phi_v = \frac{\Gamma}{2\pi} \tan^{-1}\left[\frac{x_c - x_v}{y_c - y_v}\right] \tag{8}$$

where x_c and y_c are the coordinates of the control point and x_v and y_v are the coordinates of the vortex influencing that control point. From the potential function the u and v components of velocity relative to the chord line are given by

$$u = \frac{\Gamma}{2\pi}\left[\frac{(y_c - y_v)}{(y_c - y_v)^2 + (x_c - x_v)^2}\right] \tag{9}$$

$$v = \frac{-\Gamma}{2\pi}\left[\frac{(x_c - x_v)}{(y_c - y_v)^2 + (x_c - x_v)^2}\right] \tag{10}$$

The tangential and normal velocities on the surface of the airfoil due to the vortices are then defined as

$$V_T = u \cos\theta + v \sin\theta \tag{11}$$

$$V_N = u \sin\theta - v \cos\theta \tag{12}$$

where θ is the angle of the surface, relative to the chord line, at the control point. The normal velocity is also equal to the negative of the free stream velocity component. To account for various angles of attack this equation becomes

$$V_N = - U_o \sin(\theta - \alpha) \tag{13}$$

where U_o is the free stream velocity and α is the geometric angle of attack.

Sixty panels yielded 60 linear equations such that

$$[C_{V_N}][\Gamma] = - U_o [\sin(\theta - \alpha)] \tag{14}$$

where C_{V_N} is the coefficient of normal velocity matrix, Γ is the vortex strength matrix, and $\sin(\theta - \alpha)$ is the free stream component of velocity matrix. Solving this system of linear equations simultaneously yielded the vortex strengths. The vortex strengths, Γ, were then substituted into Eqs (9) and (10) and the results were substituted into Eq (11). These equations gave the tangential velocity at each control point induced by the vortices at each panel. The V_T's were then related to the dimensionless pressure coefficients by the equation:

$$C_p = 1 - \left(\frac{V_T}{U_o}\right)^2 \tag{15}$$

In order to obtain dimensionless lift coefficients the C_p's were then integrated around the airfoil for each angle of attack.

Prediction Technique

The prediction technique developed was limited to this study. It was based on initial wind tunnel results of one airfoil and endpiece configuration and attempted to predict the results of using the other

three endpieces. This was accomplished by matching the lift coefficient results of Endpiece A and making changes in the program to simulate Endpieces B, C, and D. To match the lift coefficient test results of Endpiece A in the program, the V_T on the upper surface was controlled and thus the circulation, also. First, a particular panel control point was chosen representing the location of the actual blowing slot. Corresponding to this point the one particular linear equation of normal velocity in the matrix was rewritten as tangential velocity. It was set equal to a variable by the equation:

$$V_T = A \tag{16}$$

where A appears in the $\sin(\theta - \alpha)$ matrix. Then the vortex for that particular panel was relocated below the surface, perpendicular to the control point, and $\frac{1}{4}$ of a panel length away from it. This was done so the vortex would have more influence on that control point. Lift coefficients at angles of attack for Endpiece A were then obtained by using certain values of A. For a fixed angle of attack, the more negative A becomes, the greater the V_T. Inconsistencies in lift curve slopes between test data and the programs necessitated changing the values of A throughout a range of angles of attack, for most cases. These values of A appear in Table II. Thus, two sets of A values were obtained corresponding to the lift curve slopes of Endpiece A with no blowing and blowing at a C_μ of 0.03.

The next step was to predict the test results with Endpieces B, C, and D. To accomplish this, the program had to incorporate the changes of a new slot angle, a different trailing edge contour, and a second slot position.

The program did not have an inherent capability of a slot angle change. To simulate the more tangential blowing of Endpiece B, the values of A were made more negative and thus, V_T was increased. This was based on the assumption that the more tangential the blowing, the greater the velocity immediately downstream of the slot. These additional values of A also appear in Table II.

The circular contour of Endpiece C was put into the program by changing the paneling scheme on the trailing edge. Instead of an equation of an ellipse, an equation of a circle was used to define the surface for the last few panels. The A values obtained for Endpiece A were then used in this case to specify V_T at the slot location. These were used assuming that the amount of blowing was essentially equal for both cases.

The slot position change to 97 percent of chord in Endpiece D was accomplished by choosing a different panel and repeating the previous procedure for Endpiece A. A control point and vortex location were chosen one panel downstream of the one used for Endpiece A. Here again, to achieve lift curve slopes, the same A values obtained for Endpiece A were used to simulate the comparable amounts of blowing.

VII. Results and Discussion

General Observations

Several phenomena were observed in the wind tunnel testing of the model and endpiece configurations. The lift curves of the four endpieces without blowing were essentially equal. This similarity in lift curves appears in Figures 5 through 8 and shows that the configuration changes of each endpiece did not have a significant effect on the flow without blowing. However, with blowing, Figures 9 through 12, the endpieces had different lift curves showing the effect of the configuration changes. Also, in these curves a tendency of flow separation at higher angles of attack was observed. This stall regime generally occurred from +2 degrees to +5 degrees geometric angle of attack.

The drag curves, Figures 13 through 20, display a tendency of increasing drag towards extreme negative and positive angles of attack. These curves show that the smallest amounts of drag occurred around zero angle of attack and the largest amounts occurred towards +6 degrees angle of attack.

The lift-to-drag ratio curves, Figures 21 through 28, exhibit a tendency of decreasing L/D at the extreme negative and positive angles of attack. This was primarily due to the increasing amounts of drag in these areas.

Lift Results

The lift results are presented in Figures 5 through 12 as section lift coefficient plotted versus geometric angle of attack. The first four are for the no blowing case on each endpiece and the last four are for the blowing case on the same four endpieces.

In the no blowing cases, the C_l's of the forward splitter plate configuration increased, on the average, by 1.14 over the no splitter plate configuration. The aft splitter plate configuration's C_l's increased, on the average, by 0 87 over the no splitter plate configuration. Thus, a higher section lift coefficient was achieved by use of the forward splitter plate on each endpiece without blowing.

In the blowing cases the results were much the same. For the forward splitter plate, the C_l's increased, on the average, by 0.78 from the no splitter plate values. And the aft splitter plate C_l's increased, on the average, by only 0.69 from the no splitter plate values. Thus, the use of the splitter plate in the forward position provided the highest section lift coefficients throughout the tested range of angles of attack. In the no blowing case, these values represented a 280 percent average increase in C_l over the no splitter plate configuration and a 60 percent average increase in C_l over the aft splitter plate configuration. In the blowing case, the increases over the no splitter plate and aft splitter plate configurations were, on the average, 190 percent and 20 percent, respectively. These percentages were calculated for the middle range angles of attack.

Drag Results

The drag results are presented in Figures 13 through 20 as section total drag coefficient plotted versus geometric angle of attack. The first four are without blowing and the last four are with blowing.

In the no blowing cases, the configuration without the splitter plate provided the lowest amounts of drag. The aft splitter plate caused higher amounts of drag and the C_{d_t}'s increased an average 95 percent over the no splitter plate case. The forward splitter plate had even higher C_{d_t}'s and these were an average 130 percent higher than the no splitter plate case. These percentages were calculated for the middle range angles of attack.

The drag results in the blowing cases were somewhat less definitive. In some cases the aft splitter plate had the lowest C_{d_t}'s. This occurred around the zero angle of attack, Figures 17 and 19, and around the extreme negative angles of attack, Figure 20. The no splitter plate configuration had the least amount of drag when blowing was not used but when blowing was applied, the losses, due to the mixing of air flows below the trailing edge, caused the drag to increase. This increase was even more than that of the aft splitter plate configuration because the plate actually prevented mixing of flows and reduced these losses. However, Figures 18, 19, and 20 show that at most of the angles of attack the C_{d_t}'s were lowest for the no splitter plate case. In all cases the drag was highest for the forward splitter plate configuration.

Thus, the model and endpiece configurations achieved the lowest amounts of drag for the most part when no splitter plate was used and had the highest amounts when a splitter plate was used in the forward position.

Lift-to-Drag Ratio Results

The lift-to-drag ratio results are presented in Figures 21 through 28 as L/D plotted versus geometric angle of attack. The first four are without blowing and the last four are with blowing.

In the no blowing cases, each endpiece had a slightly different result. For Endpiece A, Fig. 21, the forward splitter plate produced the highest L/D's throughout the range of angles of attack. This was primarily due to the fact that it had much greater C_l's than the other lower surface configurations. On Endpiece B, Fig. 22, the forward splitter plate produced high L/D's at the negative angles of attack but then dropped below the higher L/D levels of the aft splitter plate and no splitter plate configurations. Up to the stall region, the highest L/D values of Endpiece C, Fig. 23, were produced with the aft splitter plate. On Endpiece D, Fig. 24, the aft splitter plate had slightly greater L/D's at the positive angles of attack but, due to the relatively small difference between these values and the forward splitter plate values, a conclusive statement about the relative merit of either configuration cannot be made. Throughout the no blowing cases, the no splitter plate configuration had the lowest L/D's, due primarily

to low C_l's. The L/D's were still on the increase at the extreme positive angles of attack thus suggesting more study at even higher angles of attack.

The lack of uniformity and definite trends in the data for the no blowing case can be attributed to significant sensitivity in the drag data reduction technique.

In the blowing cases, however, the results are more conclusive. On Endpieces A, C, and D, Figures 25, 27, and 28, the use of the aft splitter plate produced the highest L/D values. Such results were due to the fact that the plate in the aft position significantly reduced the mixing losses enough to reduce the C_{d_t} values. On Endpiece B, Figure 26, the forward splitter plate actually had slightly greater L/D's than the aft splitter plate but the relative difference was not enough to make a definite statement about this configuration.

Thus, throughout the tested range of angles of attack, the highest lift-to-drag ratios were achieved on the model and endpiece configurations with the splitter plate in the aft position. In the middle range angles of attack these L/D's of the aft splitter plate configuration represented an average increase of 37 percent over the forward splitter plate configuration and an average increase of 64 percent over the no splitter plate configuration. This was true in the blowing cases and in some of the no blowing cases. In only one case did the forward splitter plate or no splitter plate configurations exhibit significantly higher L/D values than the aft splitter plate values.

Thus, whether the airfoil had the slot located at the 96 or 97 percent chord position, at an angle of +5 or -33 degrees, or had a circular or elliptical contour, the splitter plate in the aft position provided the maximum lift-to-drag ratios. The effect of blowing was to generally increase the L/D values over those of the no blowing cases. This was true with the exception of a few cases where the secondary flow was non-uniform through the slot. Further discussion of the effects of blowing can be found in the investigation by Oxford (Ref 3).

Potential Flow Results

The results of the potential flow computer program are presented in Figures 29 through 34. The first three show the results of the lift curve matching routine and the last three show the results of the prediction technique.

The matching routine, accomplished with the values of A in Table II, assumed that potential curves would not exhibit the decrease in C_l that normally occurs when the flow separates. The values used were obtained with a linear equation and the results show somewhat linear potential flow curves that follow the test lift curves closely, up to the stall regions.

The prediction technique for each splitter plate configuration was based on the A values established for Endpiece A, with blowing. Figures 32, 33, and 34 show that when the contour was varied from

Endpiece A to C, the test lift curves changed appreciably but the potential flow curves did not. This result was possibly due to the fact that the flow in potential theory is defined to be inviscid. Under real flow conditions a circular contour makes the blowing and subsequent reattachment more effective and thus increases the C_l's, but in potential flow a contour change has an insignificant effect.

When the slot position was moved from 96 to 97 percent of the chord, Endpieces A to D, the real flow test C_l's increased appreciably. The potential flow C_l's did not increase but actually decreased at negative angles of attack. This was due to the fact that the potential flow program did not accurately simulate real flow conditions at and around the splitter plates and lower surface stagnation points.

The results of the prediction technique show that it is not useful for prediction purposes because it is constrained to this study and is based on initial wind tunnel data. A true prediction technique would not be based on initial data and would be capable of broader usage. Thus, the results imply that the program is more justifiable as a matching routine as it can match any of the lift coefficient test results.

VIII. Conclusions

A two-dimensional wind tunnel and analytic study to determine the effects of splitter plate position on trailing edge modifications of a circulation controlled airfoil resulted in the following conclusions.

1. The section lift coefficient increases as the splitter plate is moved forward toward the 95.3 percent chord position.
2. The section total drag coefficient increases as the splitter plate is moved forward toward the 95.3 percent chord position.
3. The lift-to-drag ratio is a maximum when the splitter plate is located at the 99 percent chord position.
4. The above conclusions are valid for a circulation controlled airfoil with variations in slot position, slot angle, and trailing edge contour.
5. Computer methods based on potential flow theory can be used to match lift coefficients obtained in wind tunnel testing of a circulation controlled airfoil.
6. Computer methods based solely on potential flow theory cannot be used to predict lift coefficient results obtained in wind tunnel testing of a circulation controlled airfoil.

IX. Recommendations

It is recommended that further wind tunnel tests and analytic studies be made on circulation controlled airfoils. Wind tunnel testing should include:

1. A study of the effects of a splitter plate that is free to rotate and seek its own optimal angle with the chord line.
2. A study of the effects of such a splitter plate configuration on further modifications of the trailing edge of the airfoil.

Further analytic investigation should include a potential flow study that incorporates the effects of viscosity.

Bibliography

1. Englar, Robert J. Two-Dimensional Subsonic Wind Tunnel Tests of Two 15-Percent Thick Circulation Control Airfoils. NSRDC Technical Note AL-211. Bethesda, Md.: Naval Ship Research and Development Center, 1971. AD900210.

2. Kind, R. J. and D. J. Maull. "An Experimental Investigation of a Low Speed Circulation-Controlled Elliptical Airfoil." The Aeronautical Quarterly, 19: 170-182 (May 1968).

3. Oxford, Vayl S. A Wind Tunnel Study of the Effects of Trailing Edge Modifications on the Lift-Drag Ratio of a Circulation Controlled Airfoil. Unpublished Thesis. Wright-Patterson Air Force Base, Ohio: Air Force Institute of Technology, 1975.

4. Rhynard, Wayne E. A Wind Tunnel Study of the Effects of Splitter Plate Position and Angle on the Lift-Drag Ratio of a Circulation Controlled Elliptical Airfoil. Unpublished Thesis. Wright-Patterson Air Force Base, Ohio: Air Force Institute of Technology, 1974.

5. Stevenson, Thomas A. A Wind Tunnel Study of the Lift-Drag Ratio on a Cambered Circulation Controlled Airfoil. Unpublished Thesis. Wright-Patterson Air Force Base, Ohio: Air Force Institute of Technology, 1974.

6. Williams, Robert M. and H. J. Howe. Two-Dimensional Subsonic Wind Tunnel Tests on a 20 Percent Thick, 5 Percent Cambered Circulation Control Airfoil. NSRDC Technical Note AL-176, Washington, D. C.: Naval Ship Research and Development Center, 1970. AD877764.

Appendix A

Apparatus

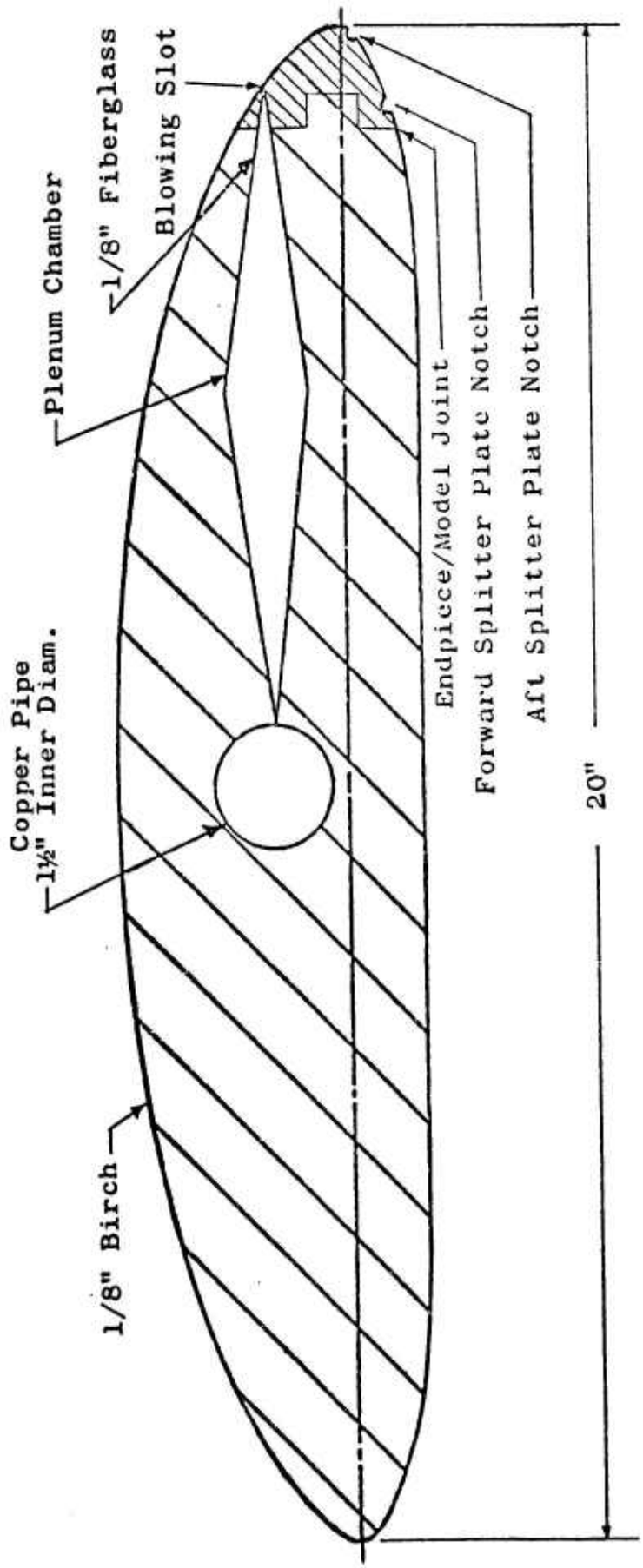

Fig. 1 Cross Section of the Airfoil With Endpiece Attached

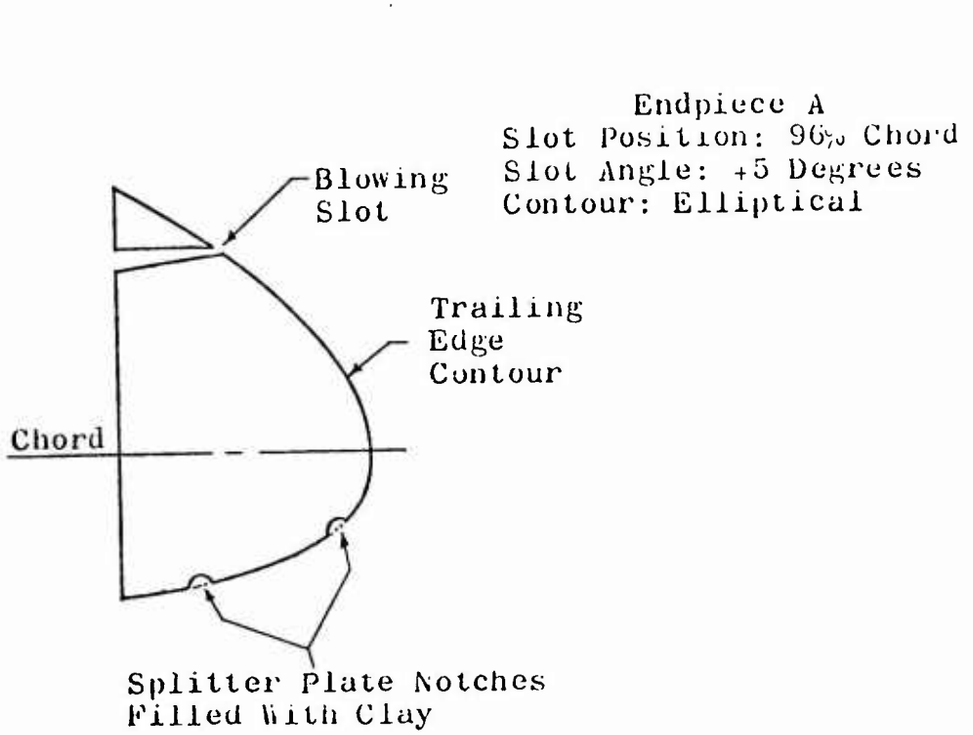

Scale: 1"=1"

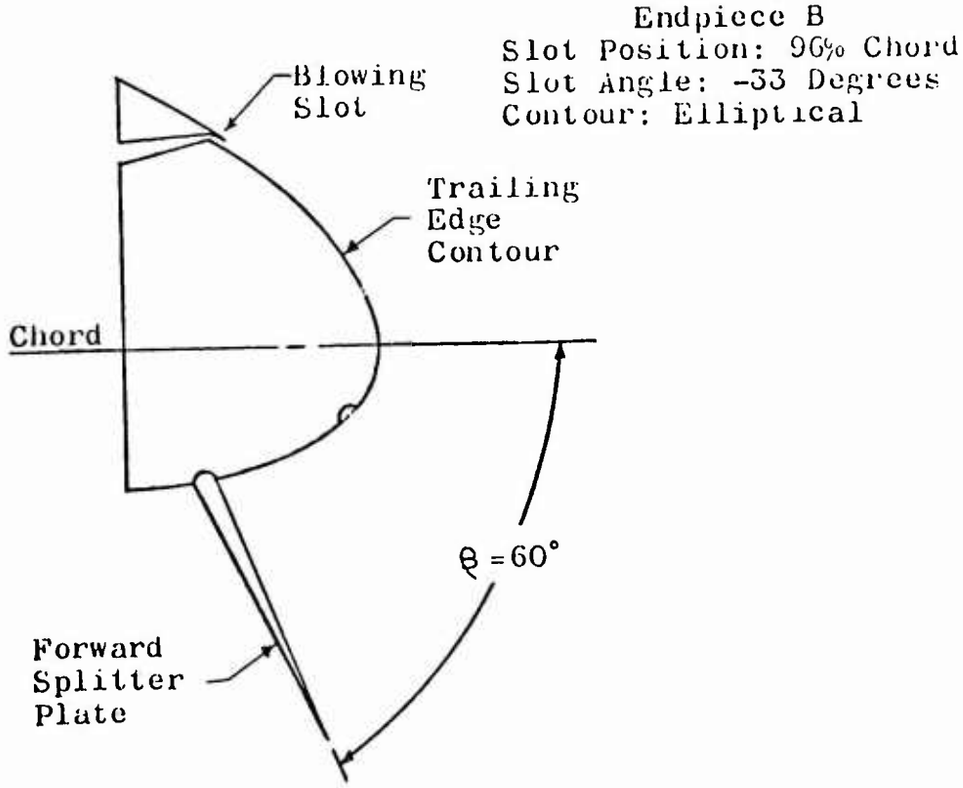

Fig. 2 Trailing Edge Configurations of Endpieces A and B

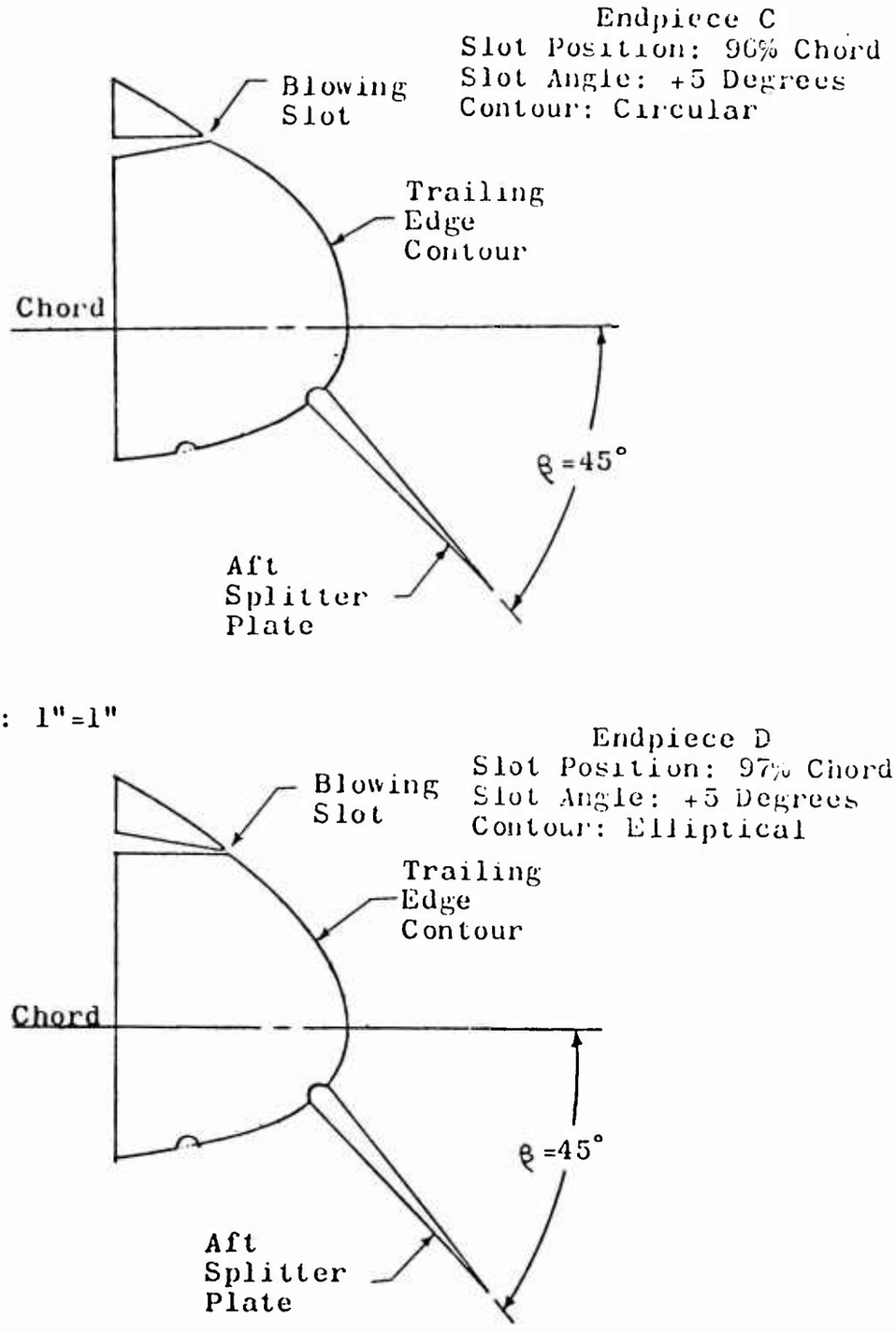

Fig. 3 Trailing Edge Configurations of Endpieces C and D

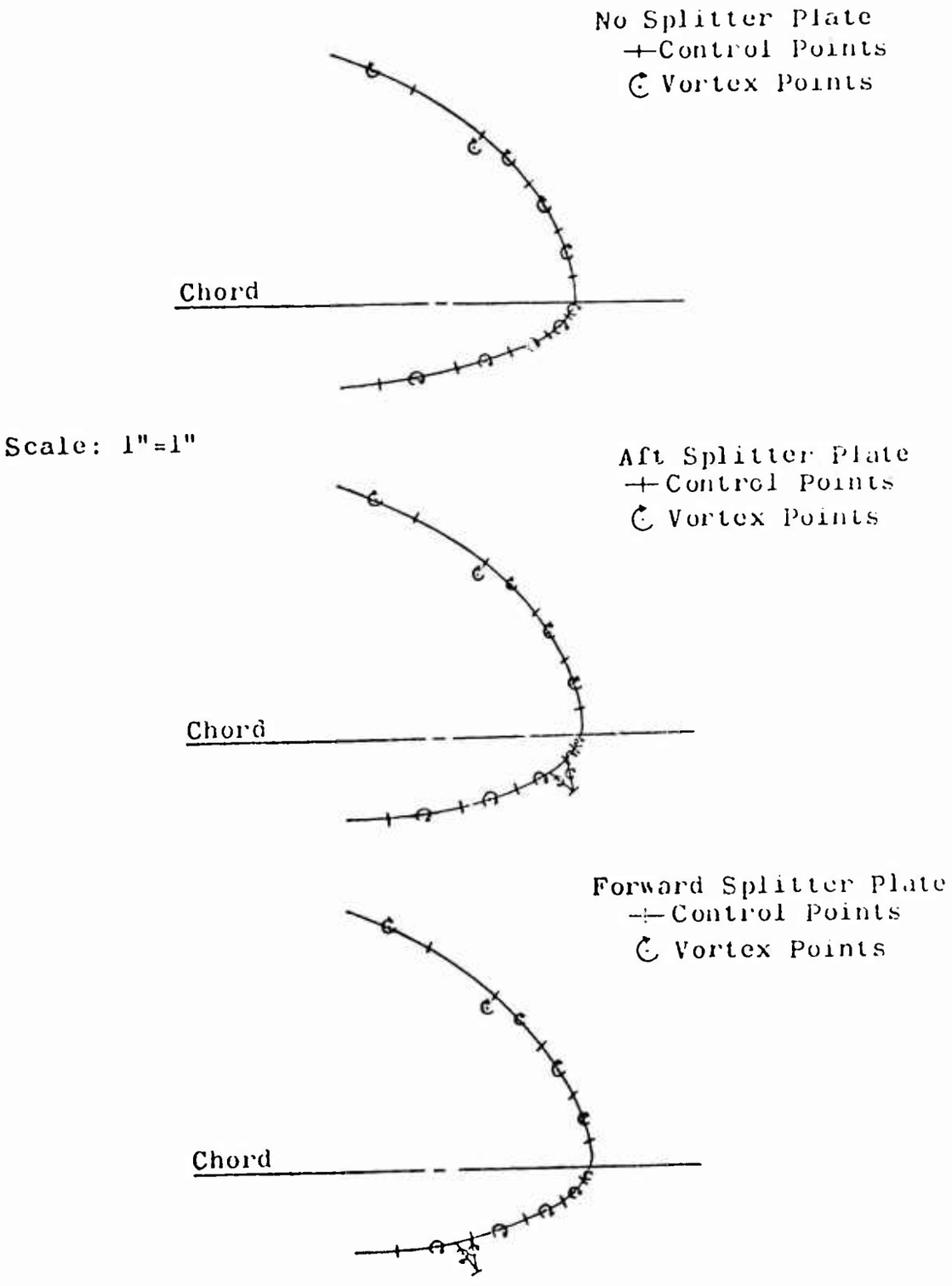

Fig. 4 The Three Trailing Edge Configurations Used on Endpiece A in the Potential Flow Program

Appendix B

Data

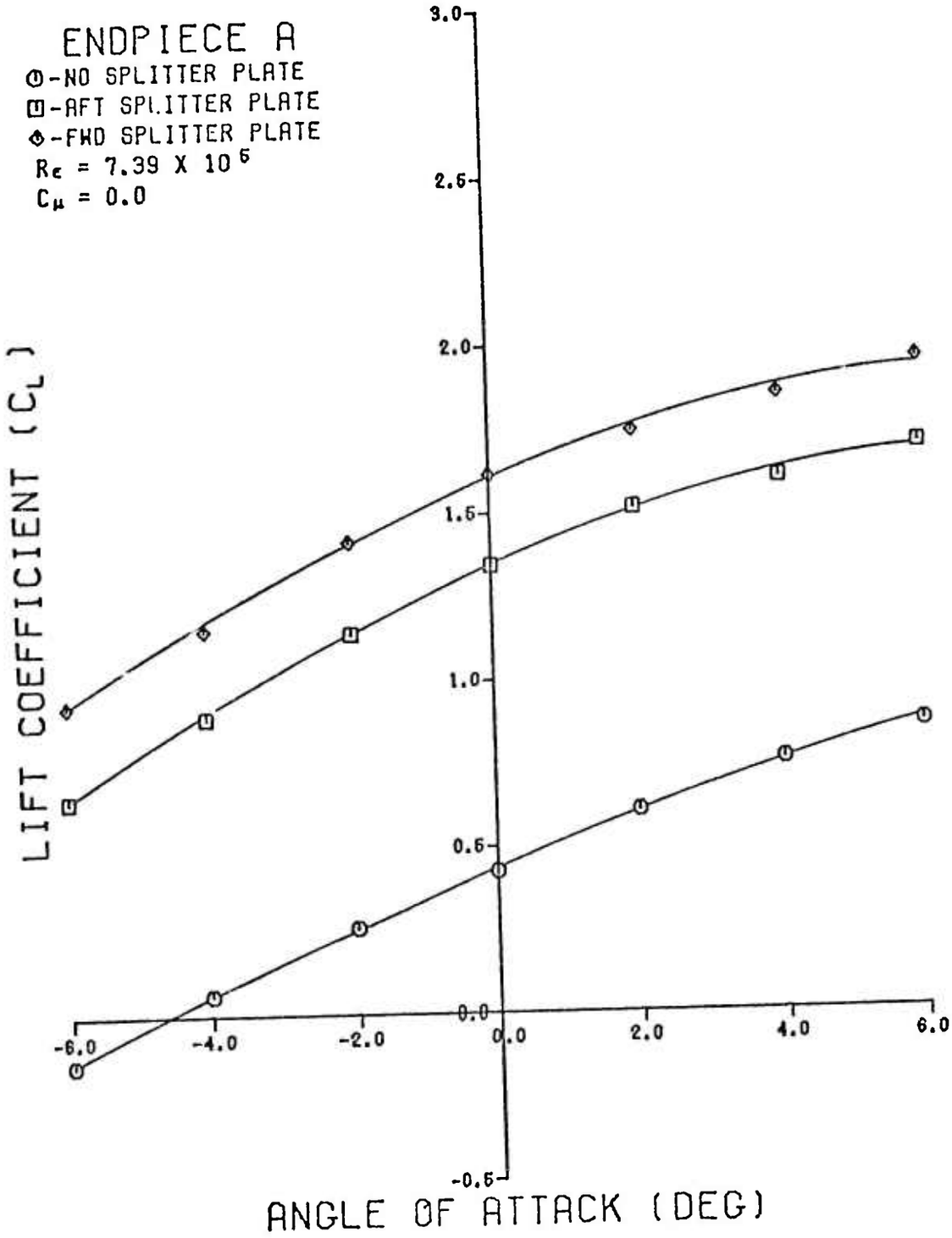

Fig. 5 The Change in C_l vs α Due to the Different Splitter Plate Configurations on Endpiece A, Without Blowing

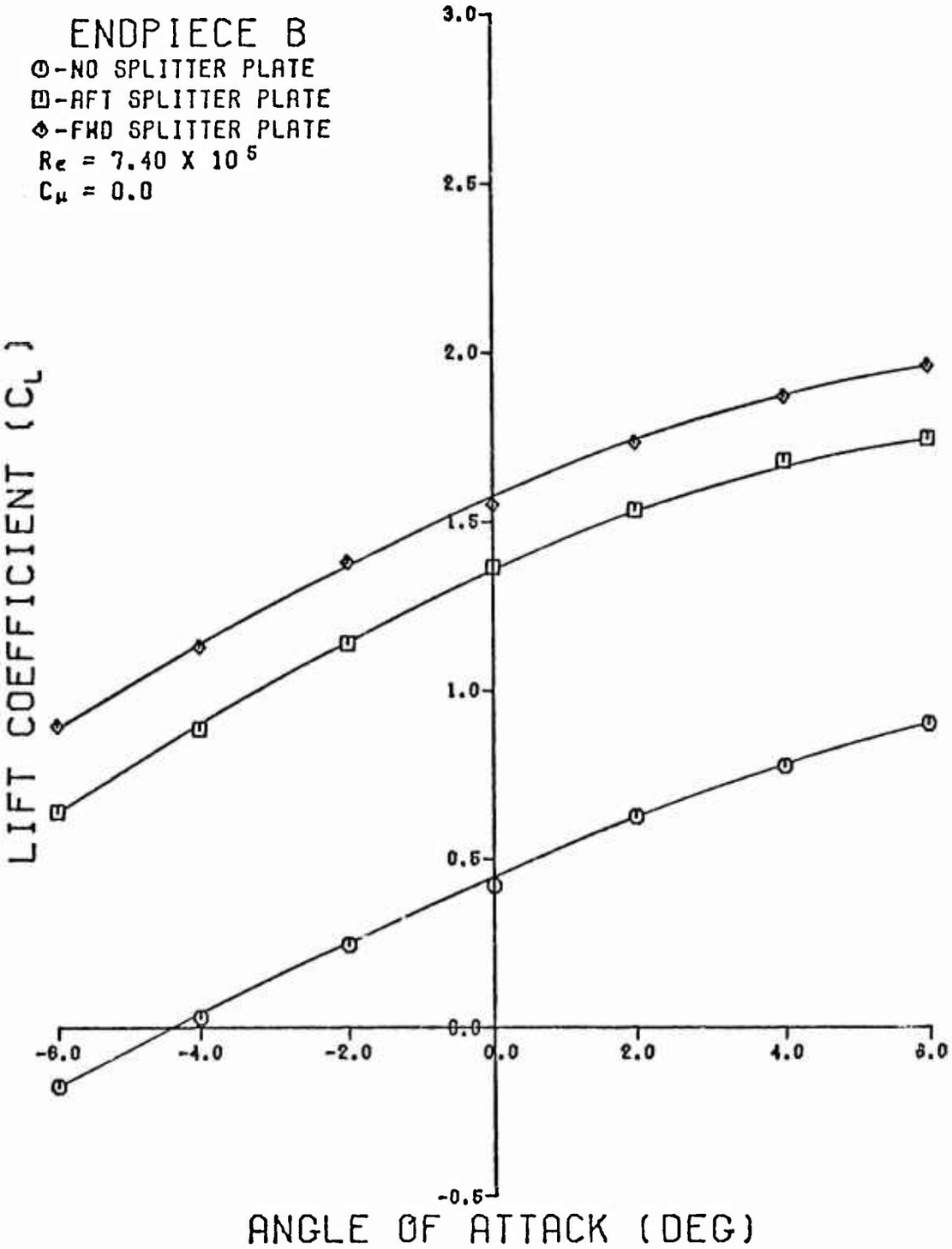

Fig. 6 The Change in C_l vs α Due to the Different Splitter Plate Configurations on Endpiece B, Without Blowing

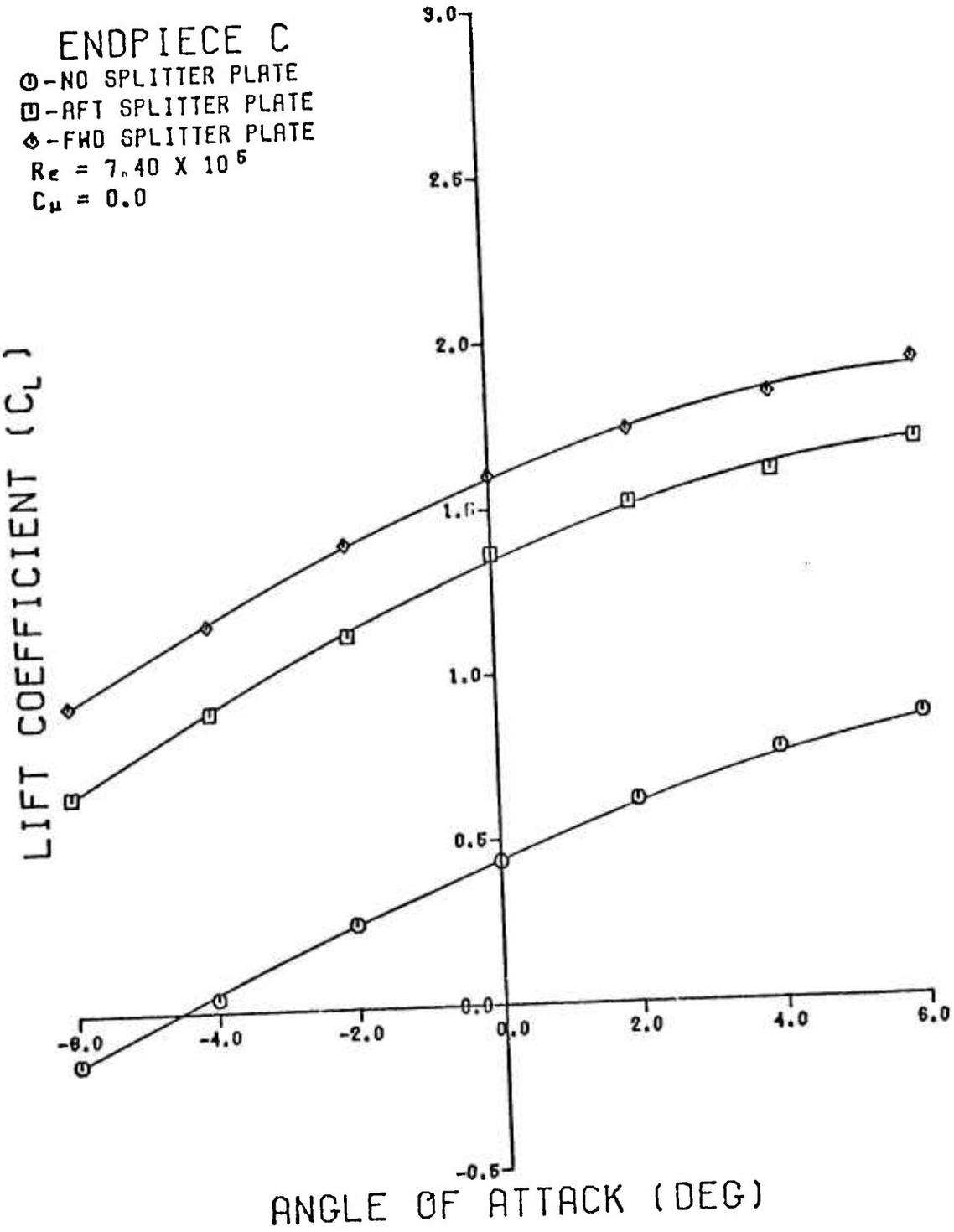

Fig. 7 The Change in C_l vs α Due to the Different Splitter Plate Configurations on Endpiece C, Without Blowing

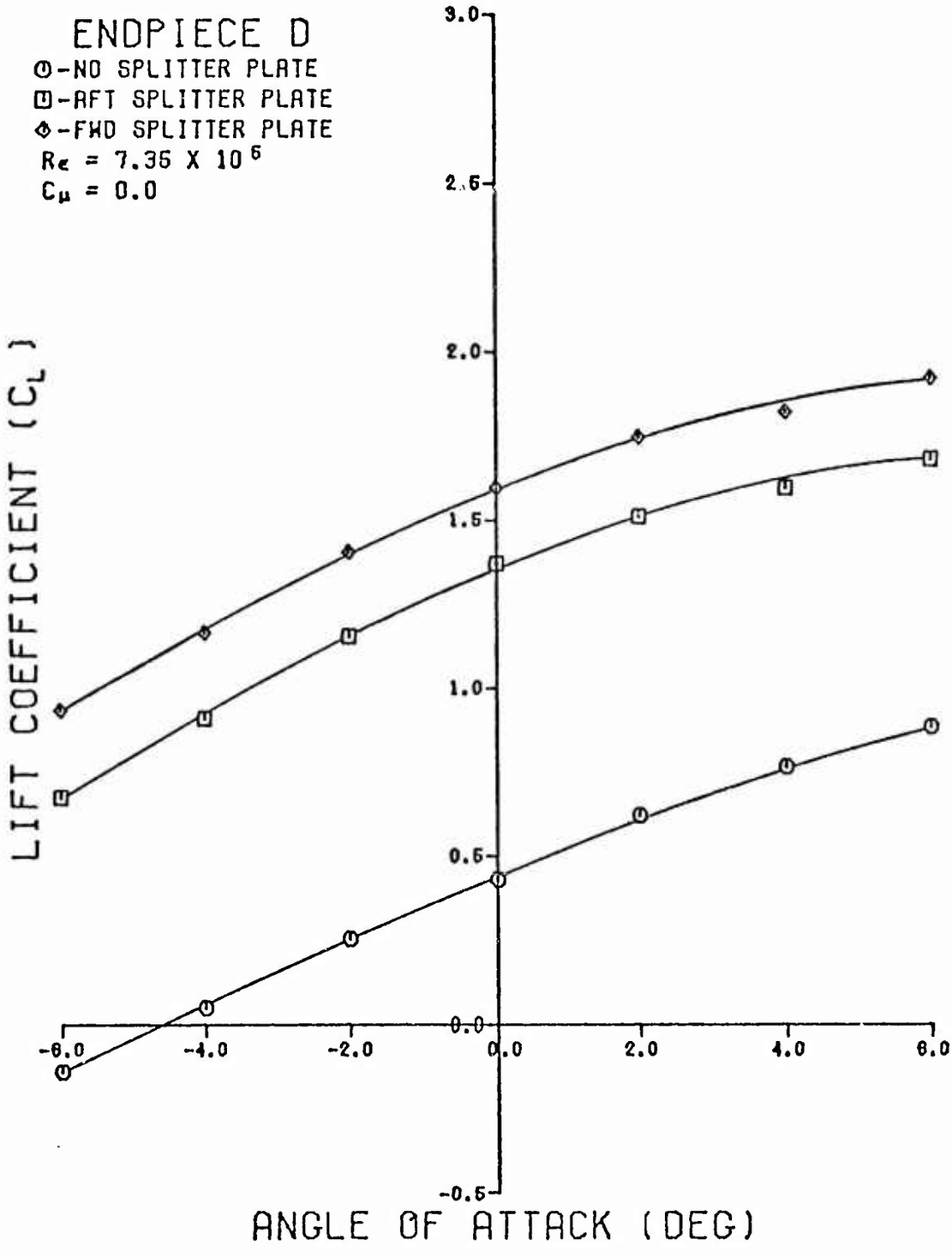

Fig. 8 The Change in C_l vs α Due to the Different Splitter Plate Configurations on Endpiece D, Without Blowing

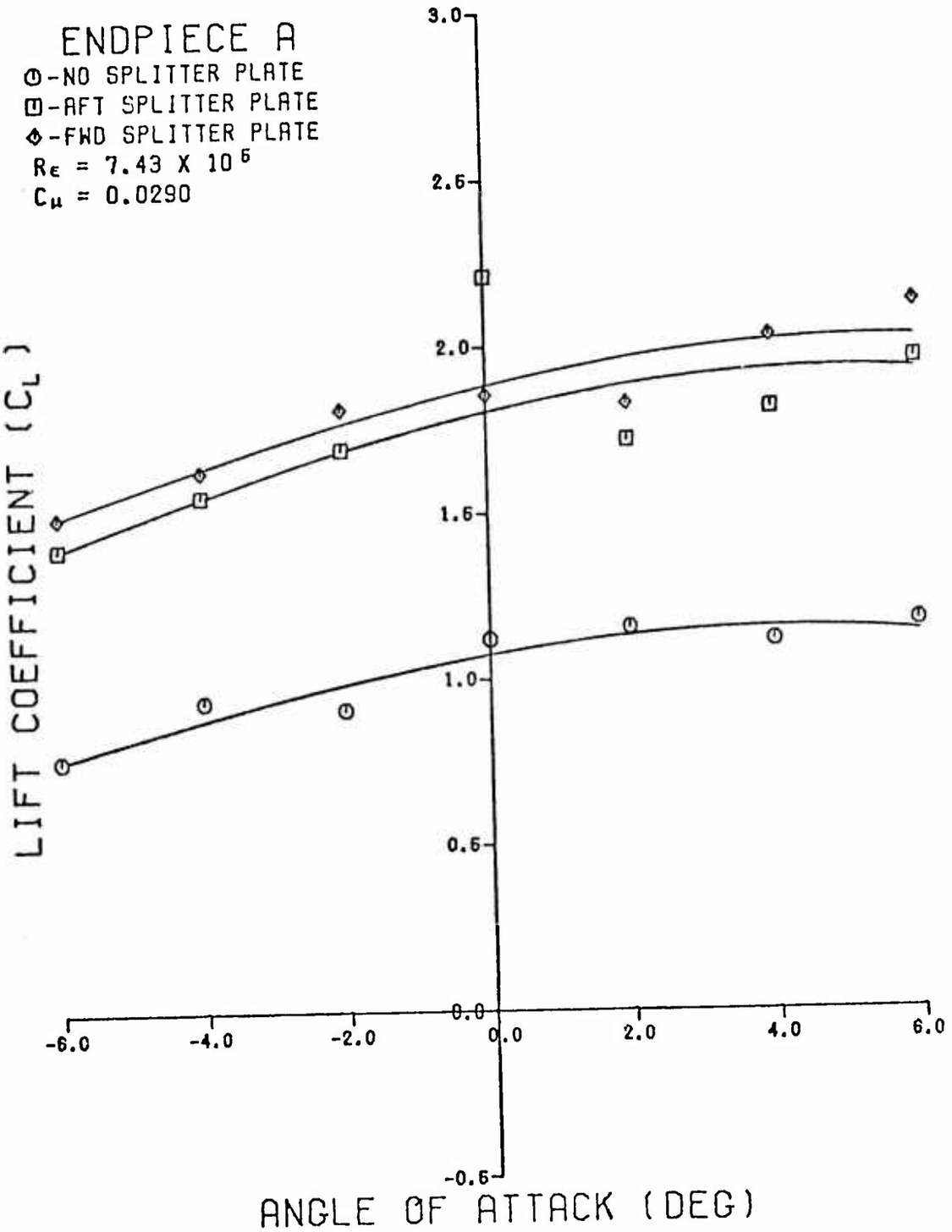

Fig. 9 The Change in C_l vs α Due to the Different Splitter Plate Configurations on Endpiece A, With Blowing

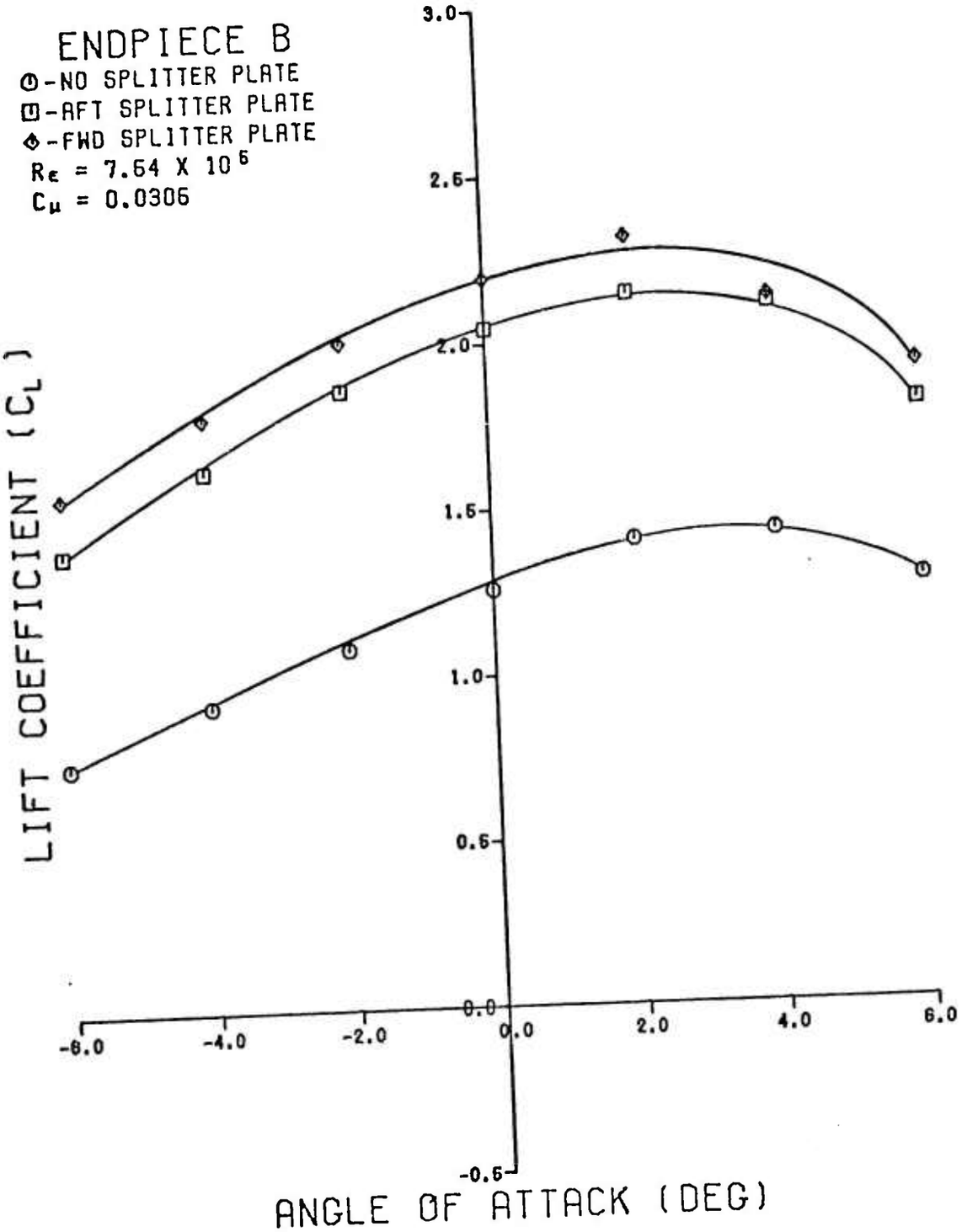

Fig. 10 The Change in C_l vs α Due to the Different Splitter Plate Configurations on Endpiece B, With Blowing

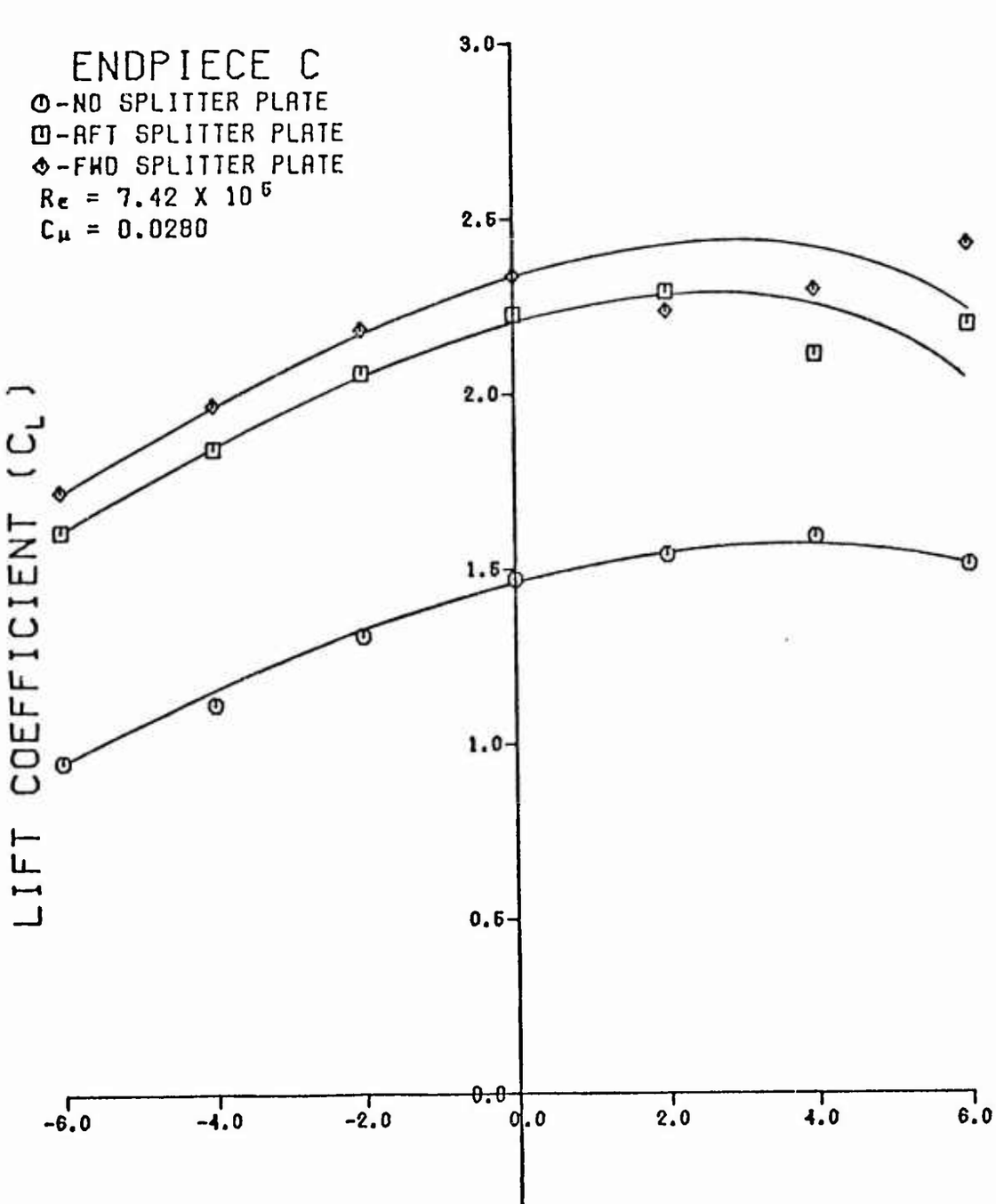

Fig. 11 The Change in C_l vs α Due to the Different Splitter Plate Configurations on Endpiece C, With Blowing

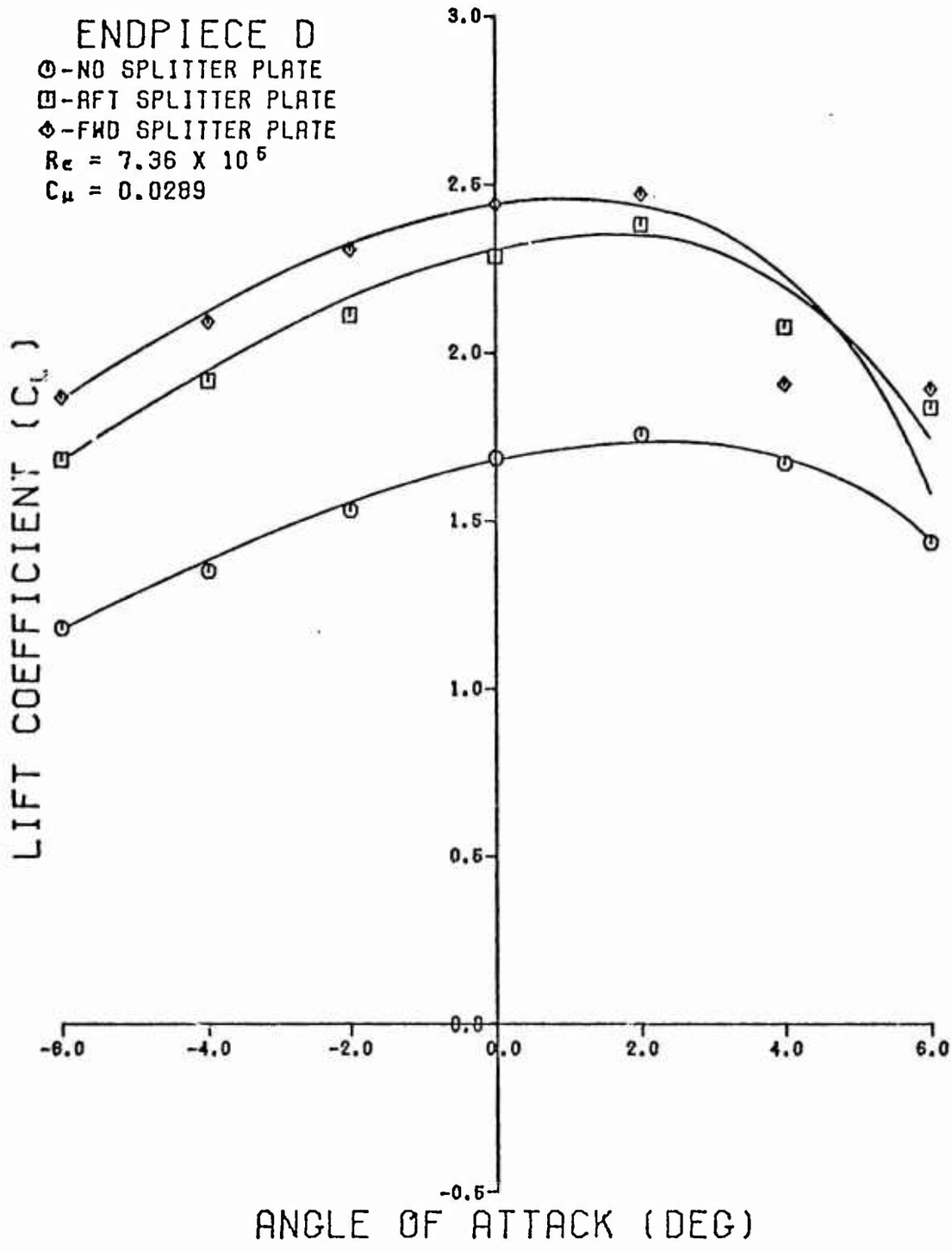

Fig. 12 The Change in C_l vs α Due to the Different Splitter Plate Configurations on Endpiece D, With Blowing

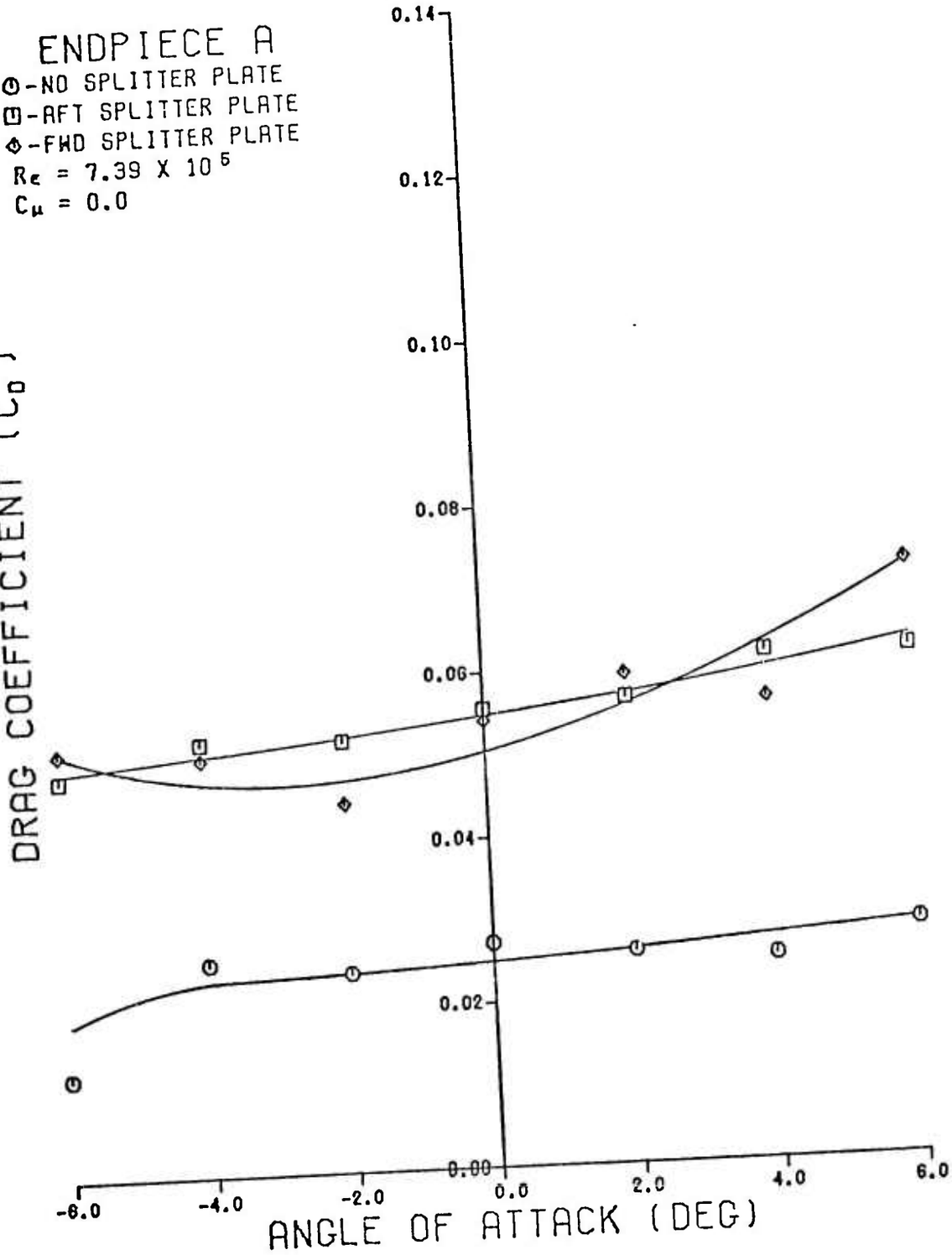

Fig. 13 The Change in C_{d_t} vs α Due to the Different Splitter Plate Configurations on Endpiece A, Without Blowing

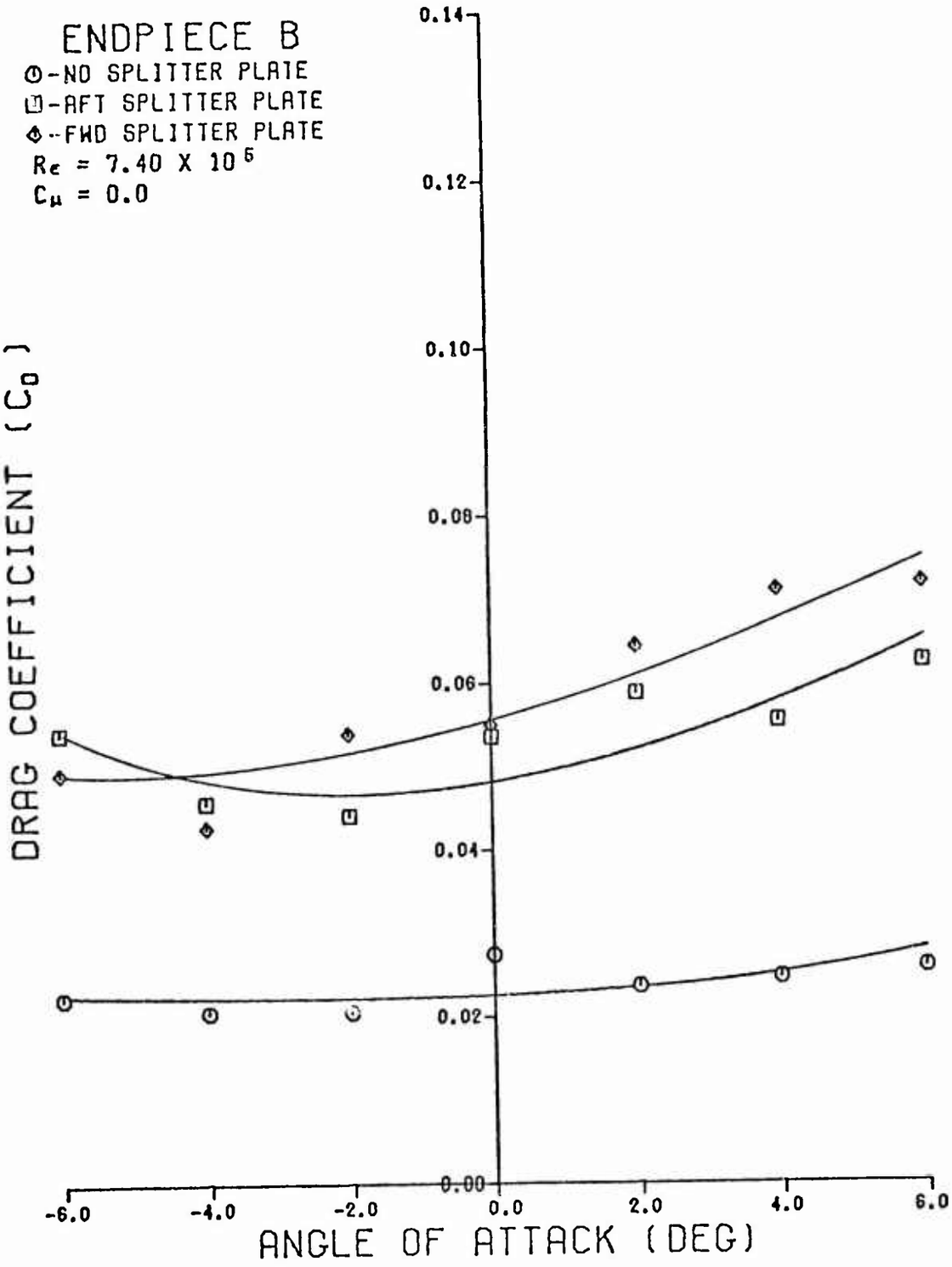

Fig. 14 The Change in C_{d_t} vs α Due to the Different Splitter Plate Configurations on Endpiece B, Without Blowing

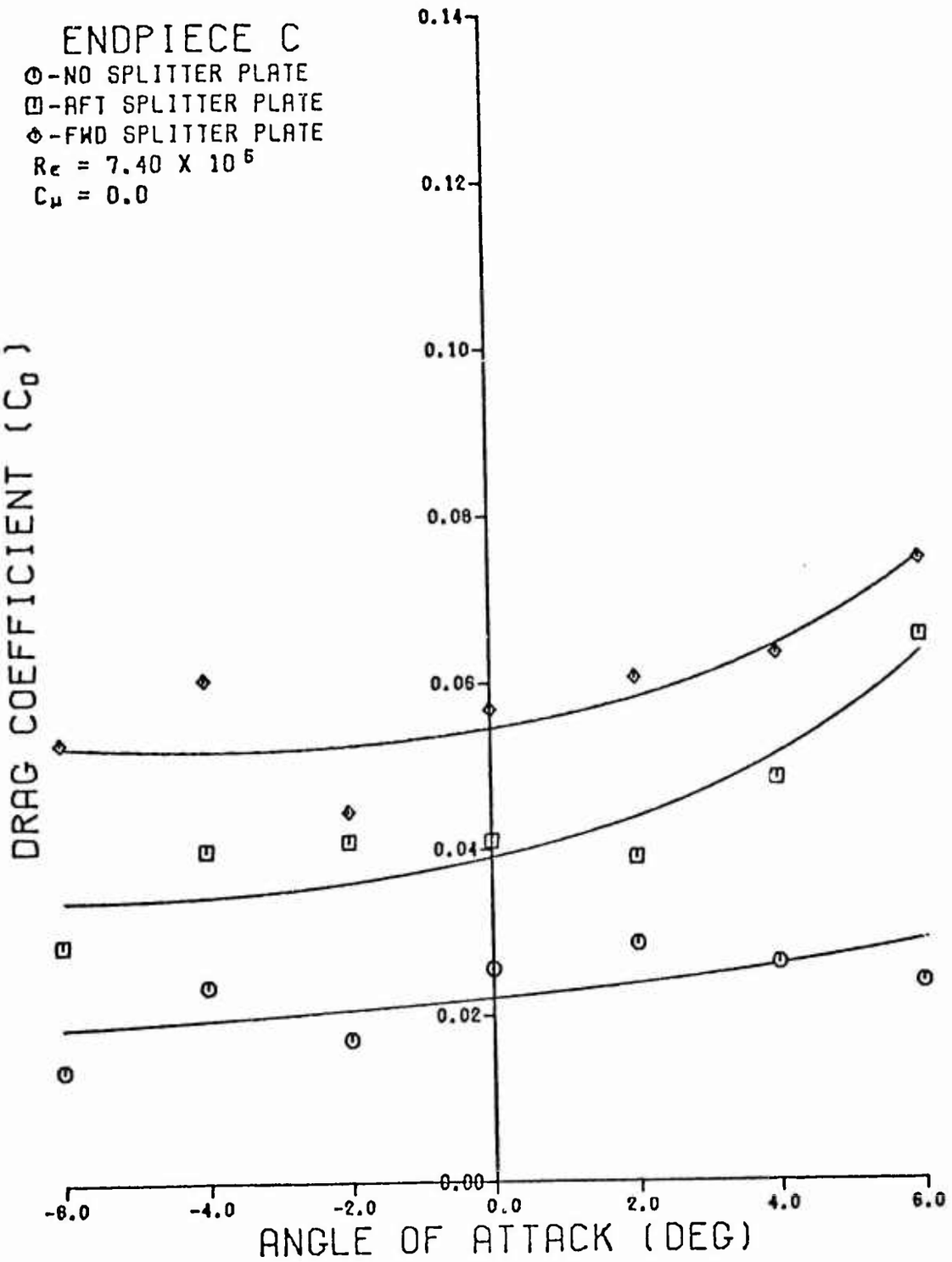

Fig. 15 The Change in C_{d_t} vs α Due to the Different Splitter Plate Configurations on Endpiece C, Without Blowing

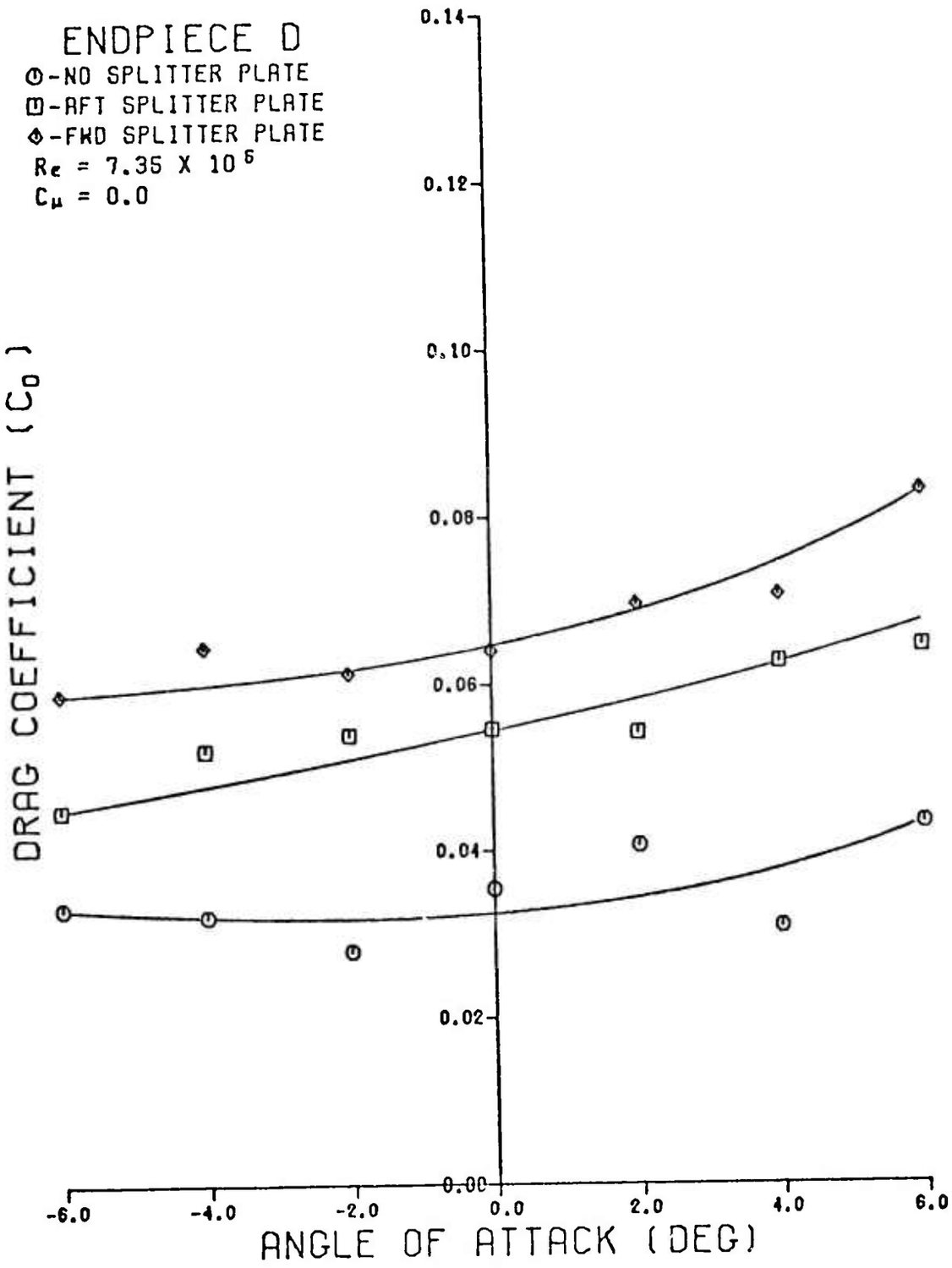

Fig. 16 The Change in C_{d_t} vs α Due to the Different Splitter Plate Configurations on Endpiece D, Without Blowing

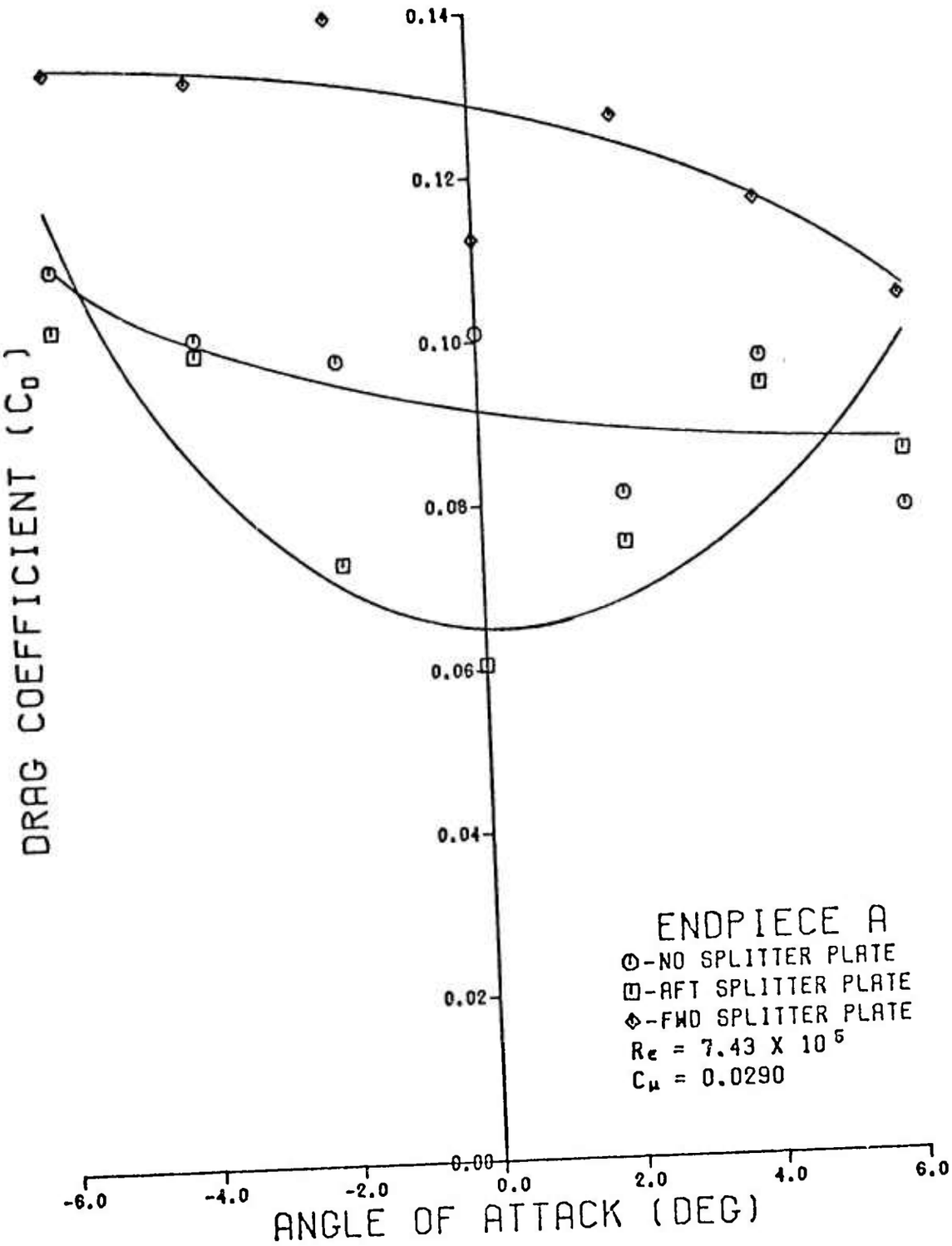

Fig. 17 The Change in C_{d_t} vs α Due to the Different Splitter Plate Configurations on Endpiece A, With Blowing

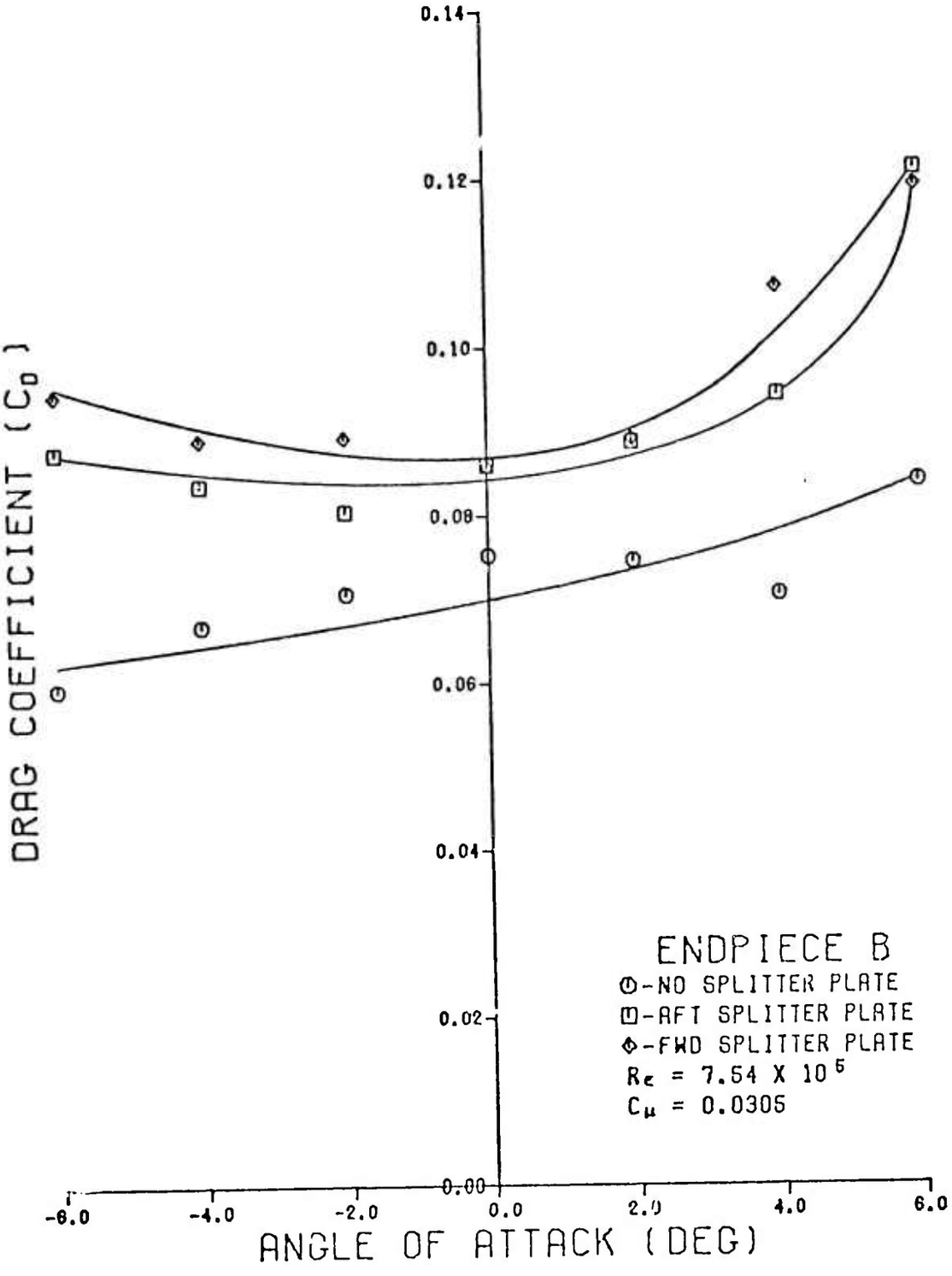

Fig. 18 The Change in C_{d_t} vs α Due to the Different Splitter Plate Configurations on Endpiece B, With Blowing

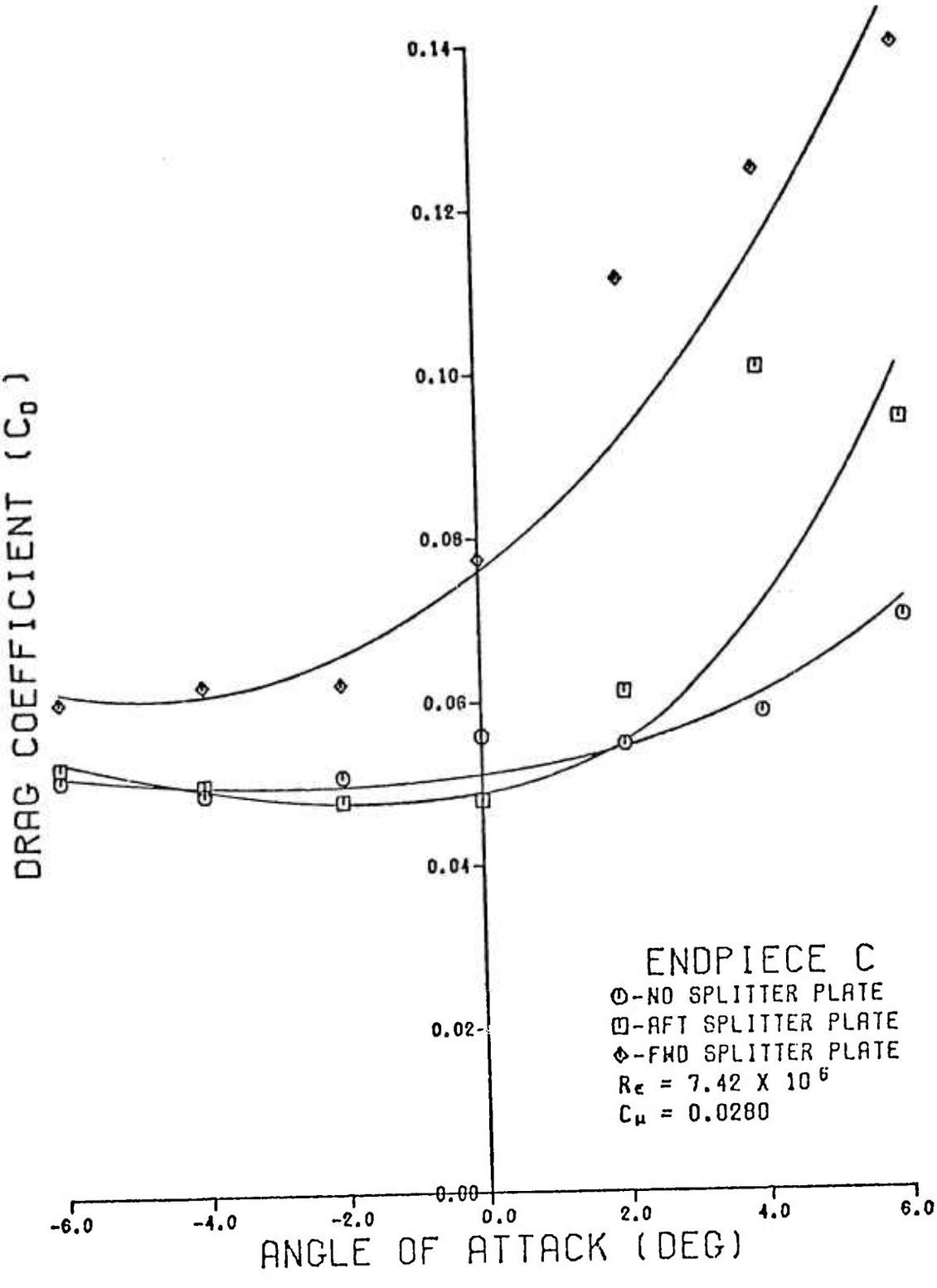

Fig. 19 The Change in C_{d_t} vs α Due to the Different Splitter Plate Configurations on Endpiece C, With Blowing

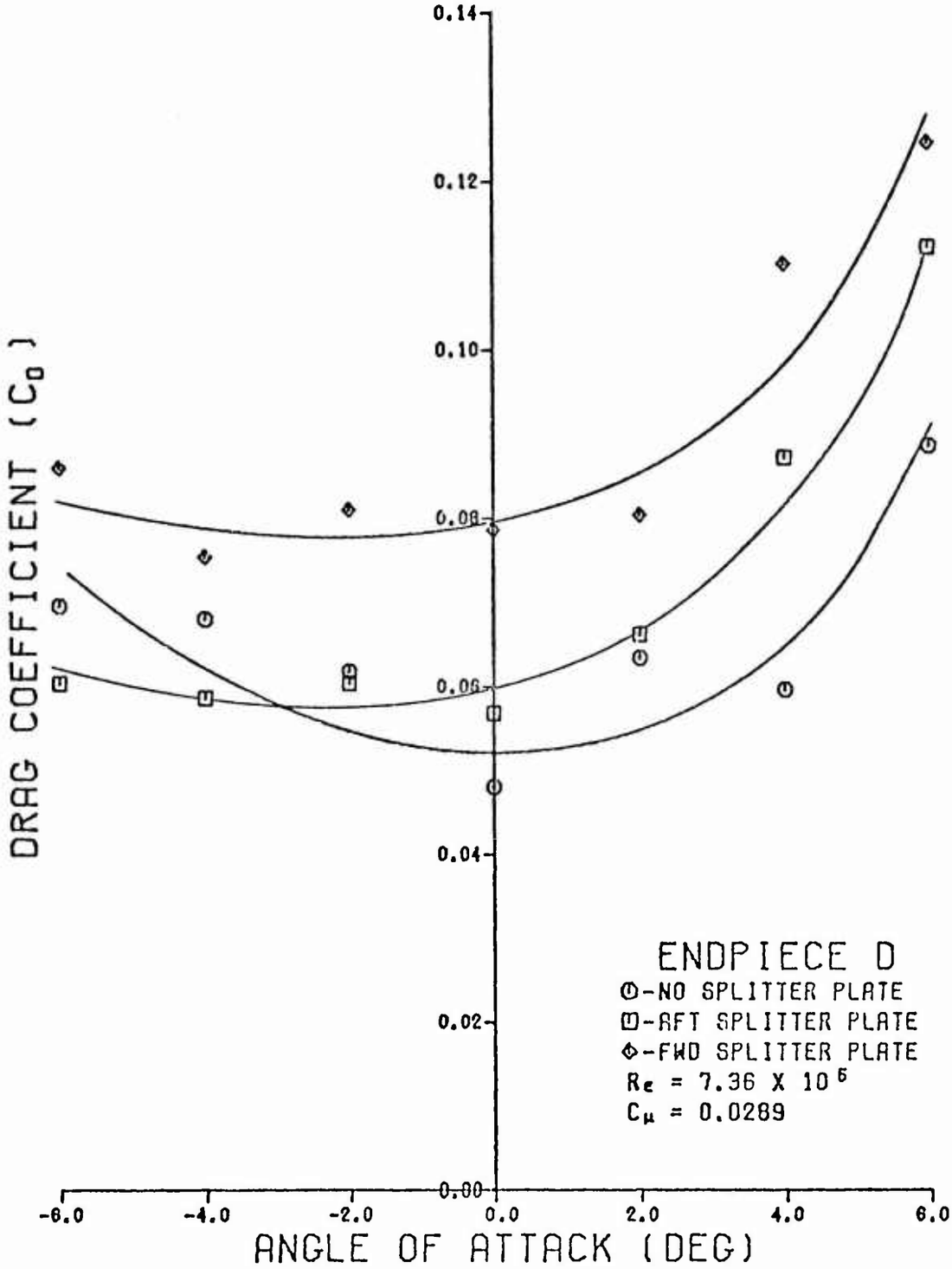

Fig. 20 The Change in C_{d_t} vs α Due to the Different Splitter Plate Configurations on Endpiece D, With Blowing

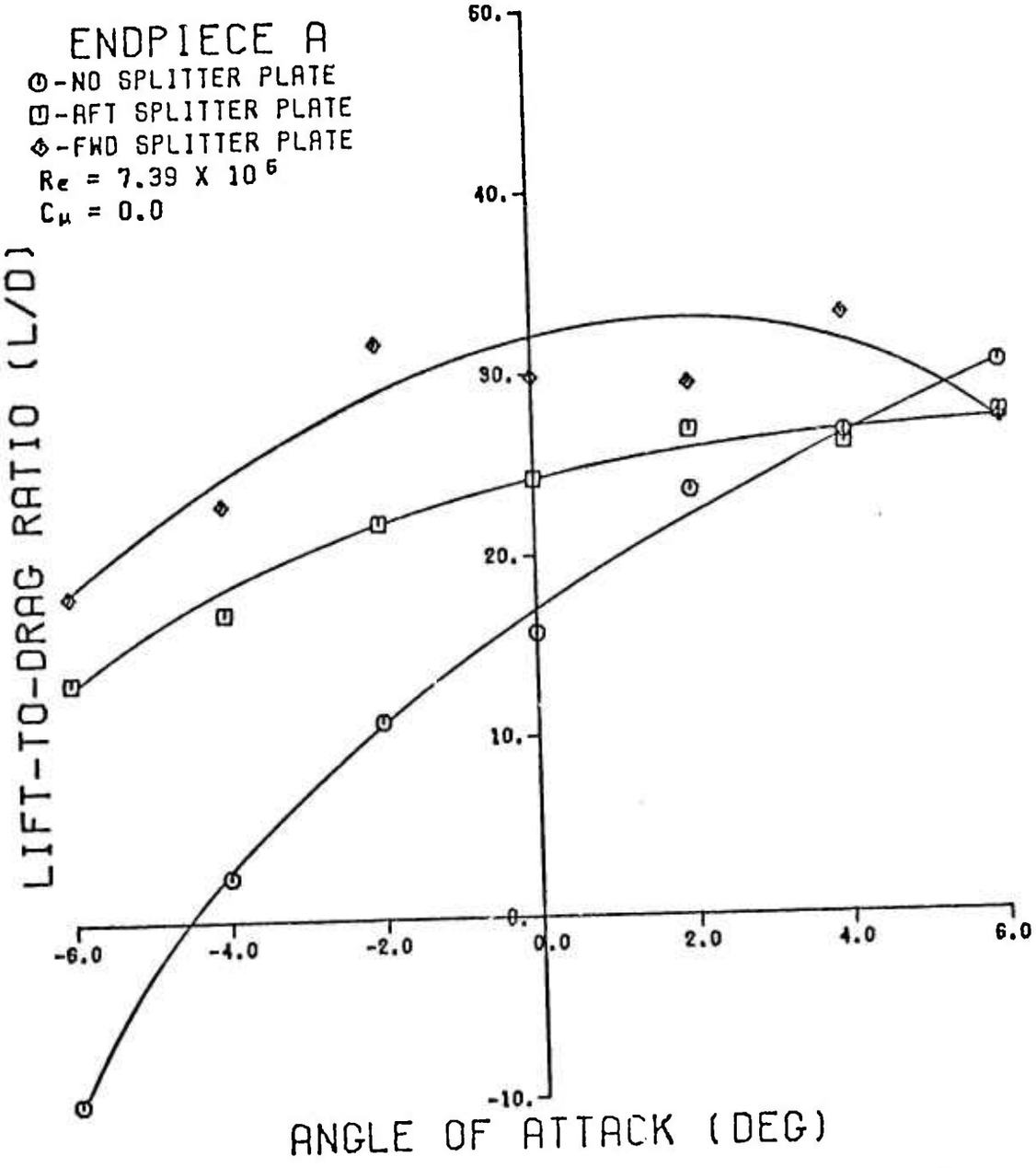

Fig. 21 The Change in L/D vs α Due to the Different Splitter Plate Configurations on Endpiece A, Without Blowing

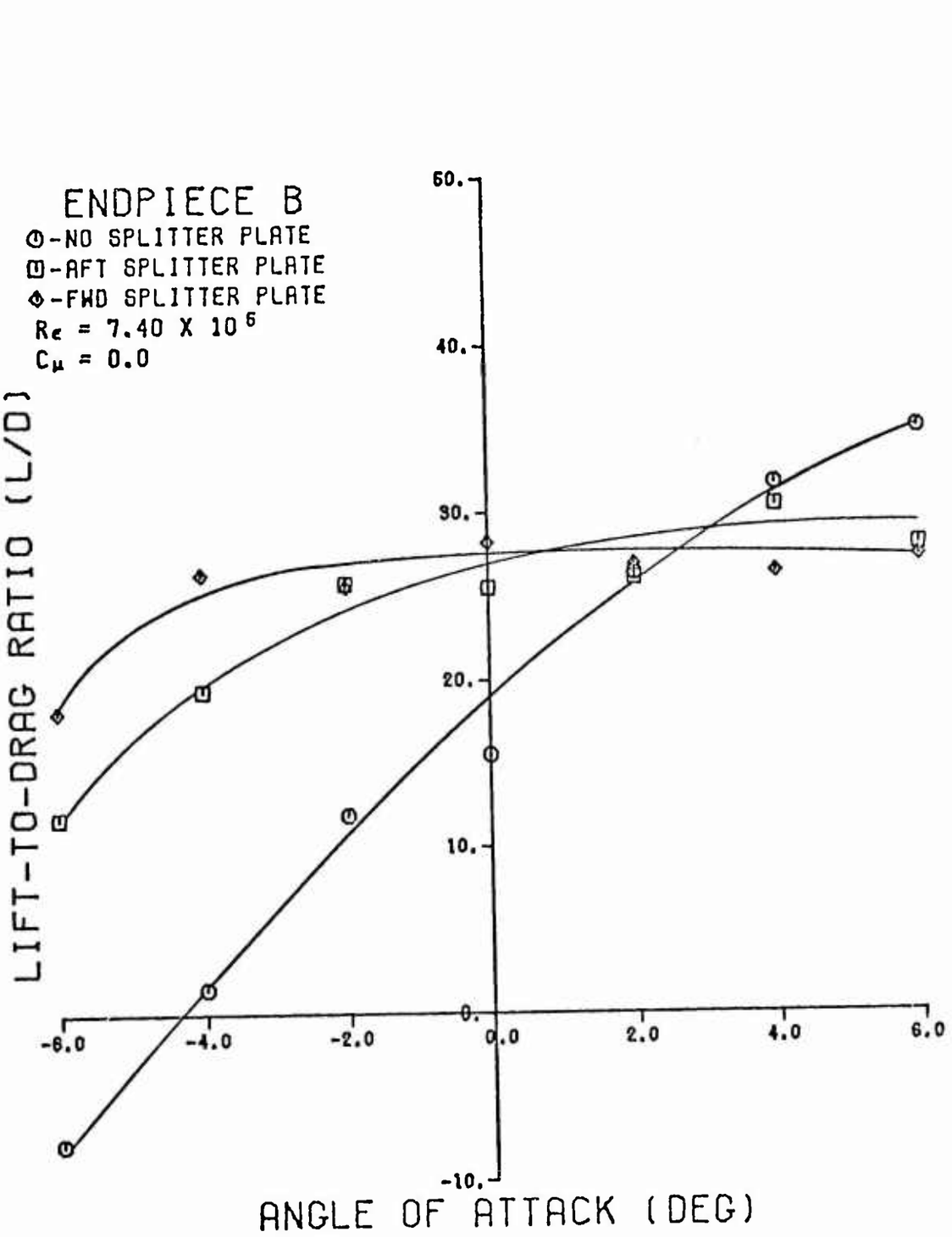

Fig. 22 The Change in L/D vs α Due to the Different Splitter Plate Configurations on Endpiece B, Without Blowing

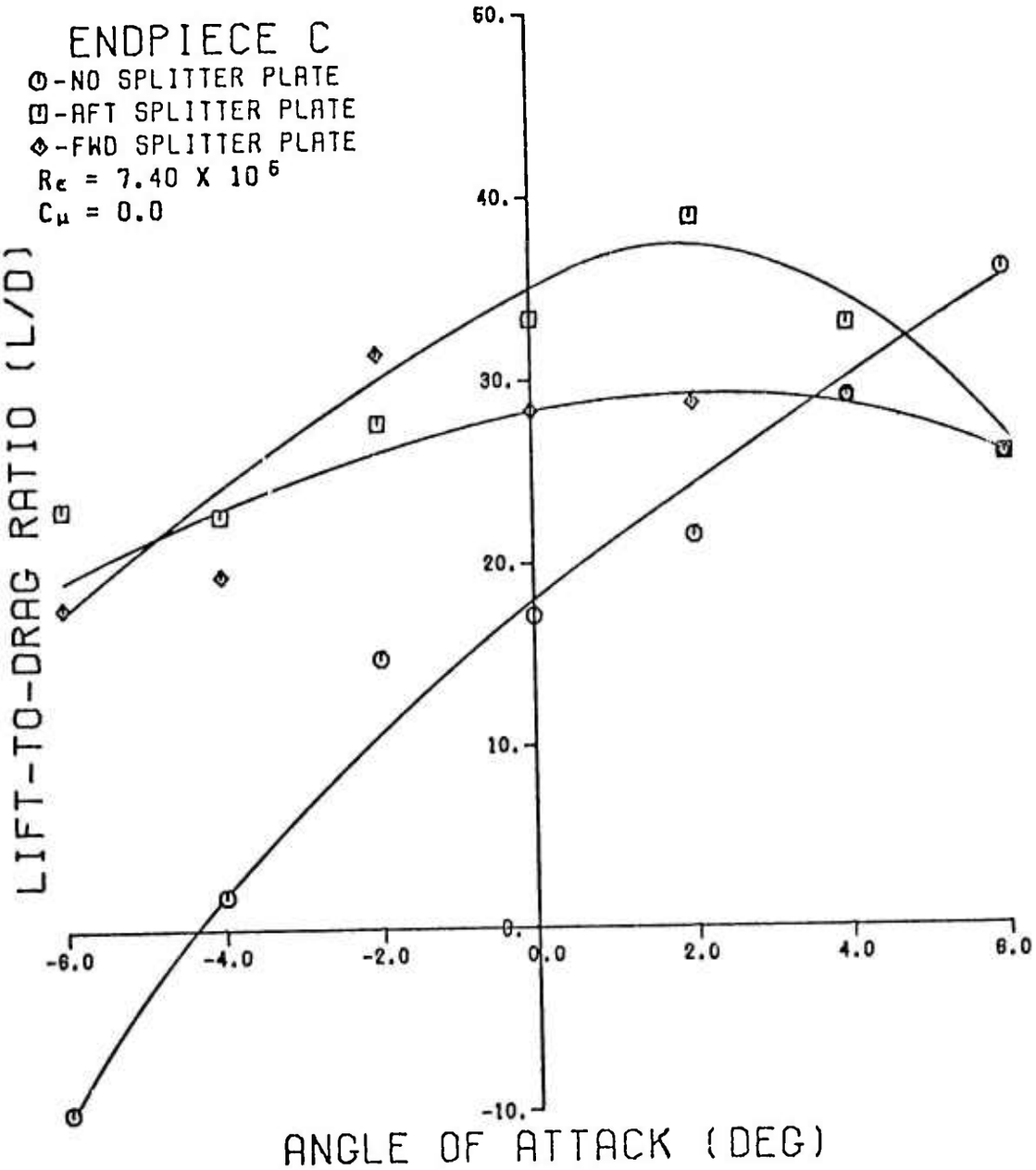

Fig. 23 The Change in L/D vs α Due to the Different Splitter Plate Configurations on Endpiece C, Without Blowing

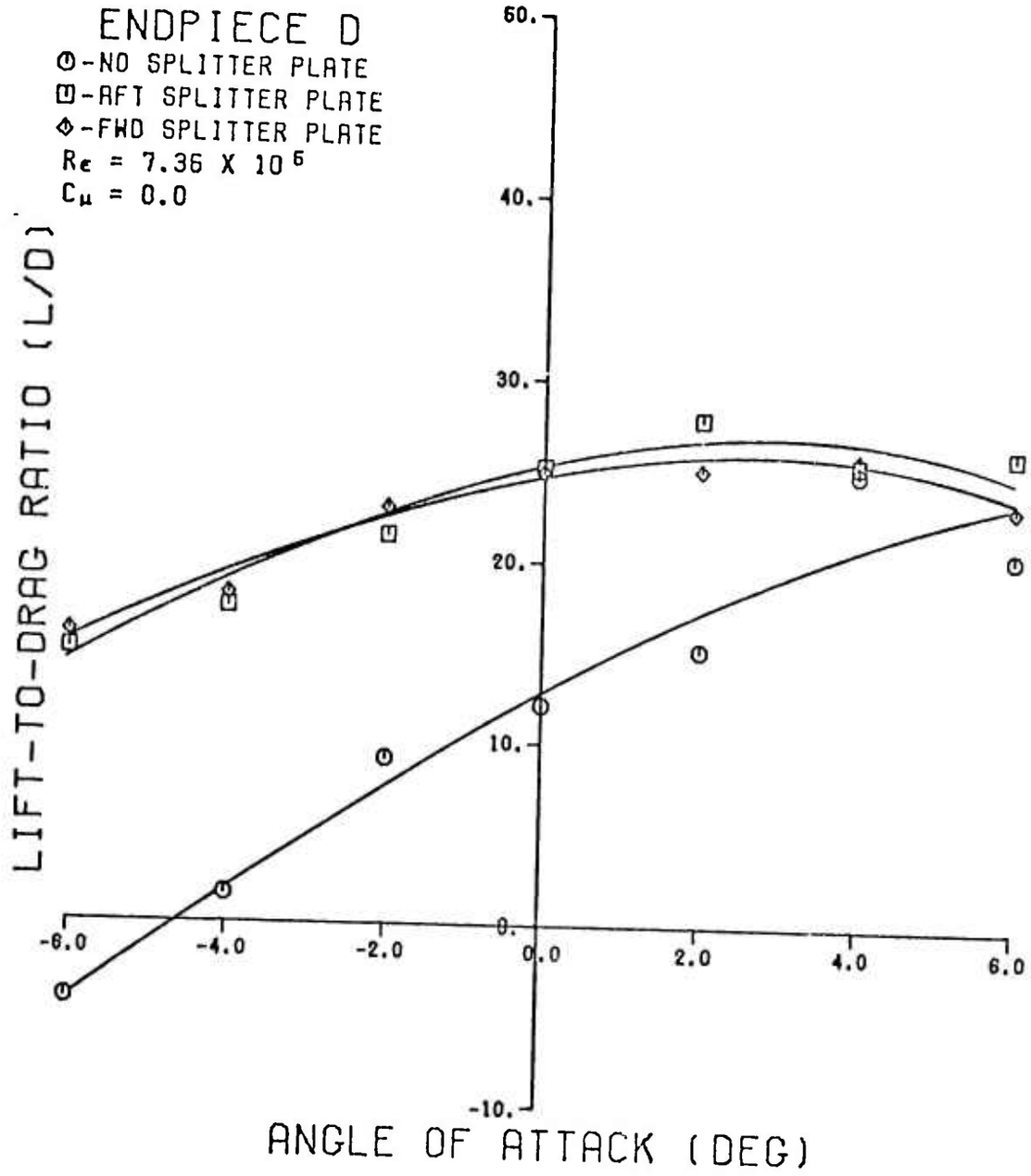

Fig. 24 The Change in L/D vs α Due to the Diff rent Splitter Plate Configurations on Endpiece D, Without Blowing

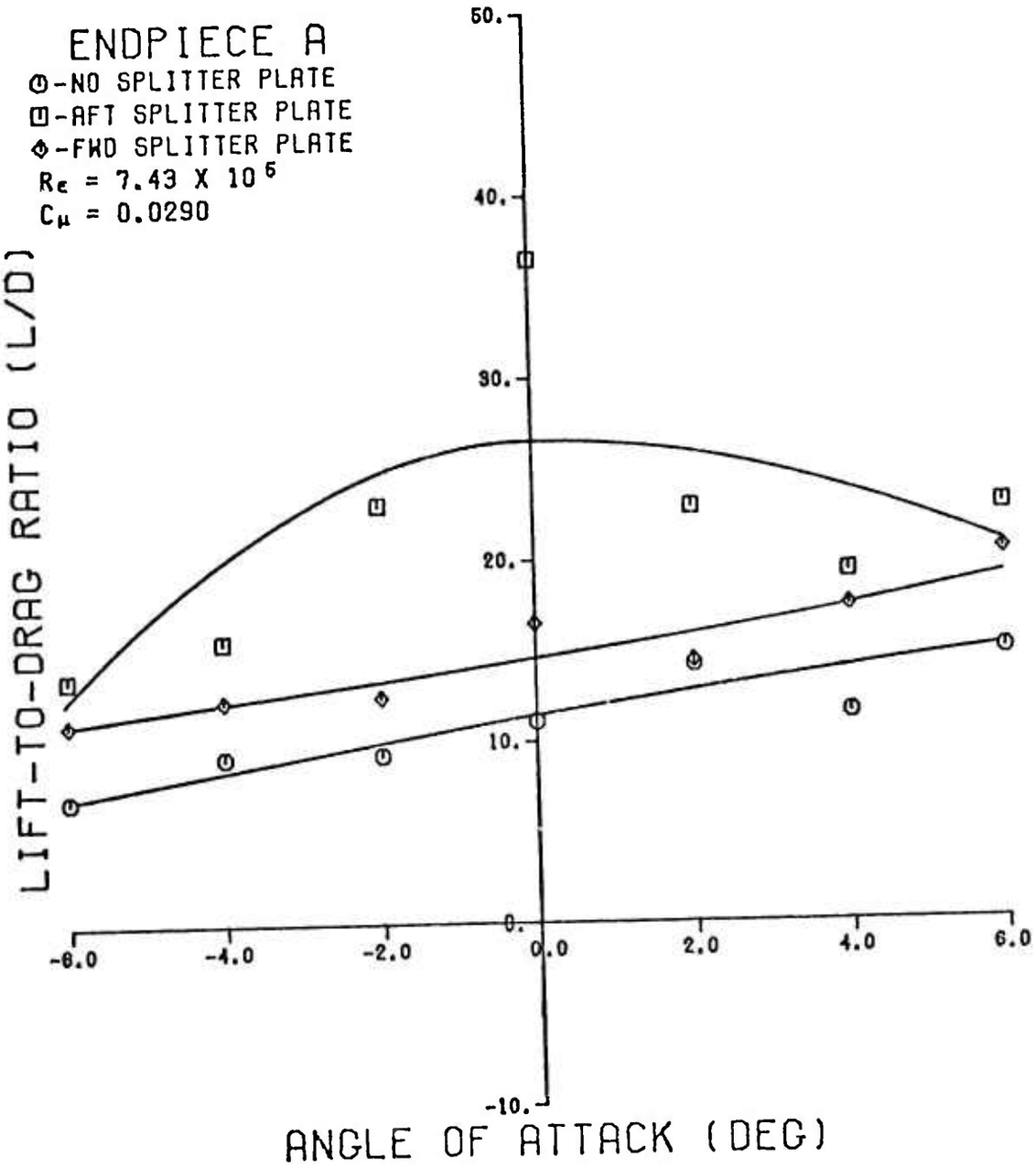

Fig. 25 The Change in L/D vs α Due to the Different Splitter Plate Configurations on Endpiece A, With Blowing

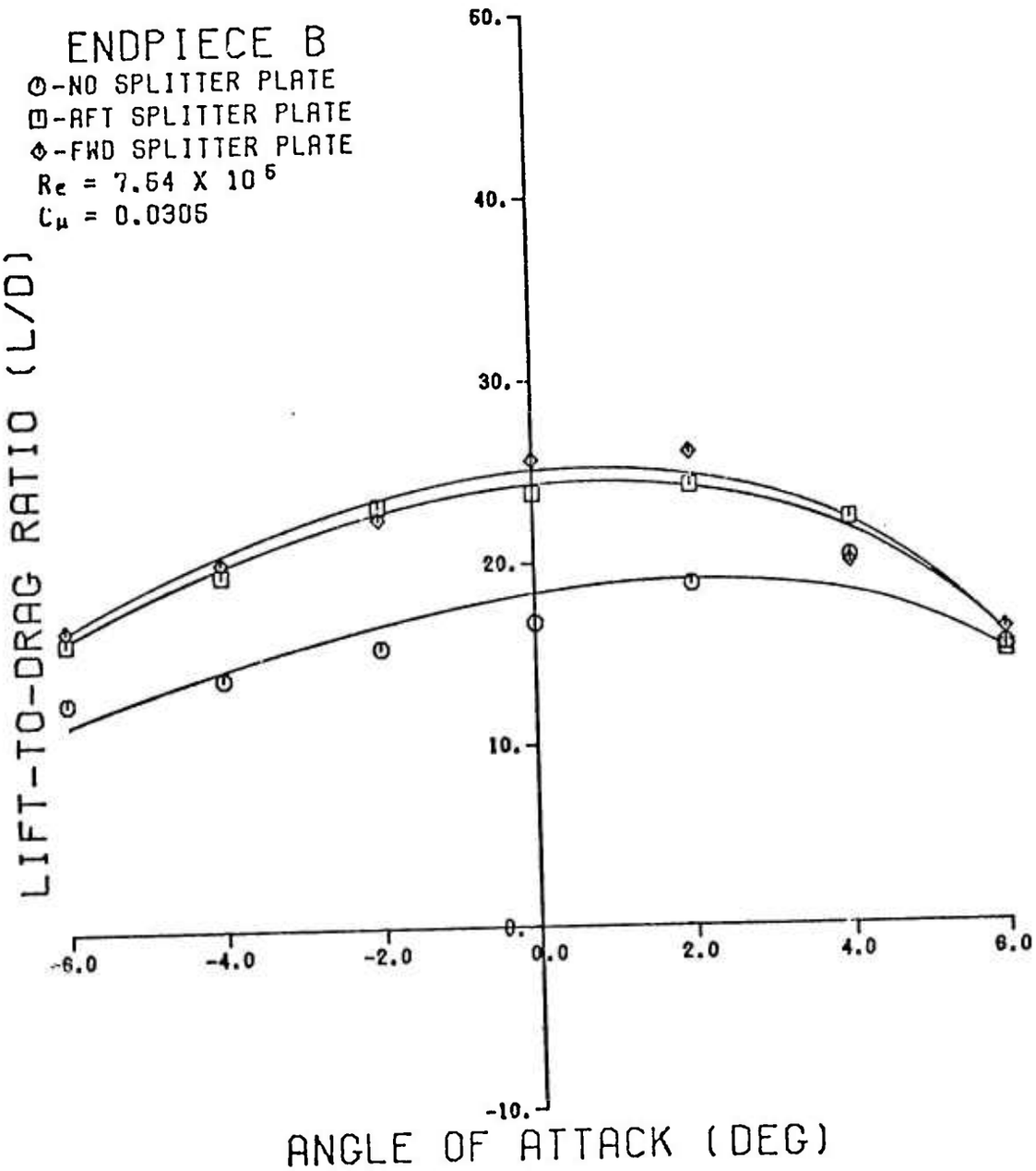

Fig. 26 The Change in L/D vs α Due to the Different Splitter Plate Configurations on Endpiece B, With Blowing

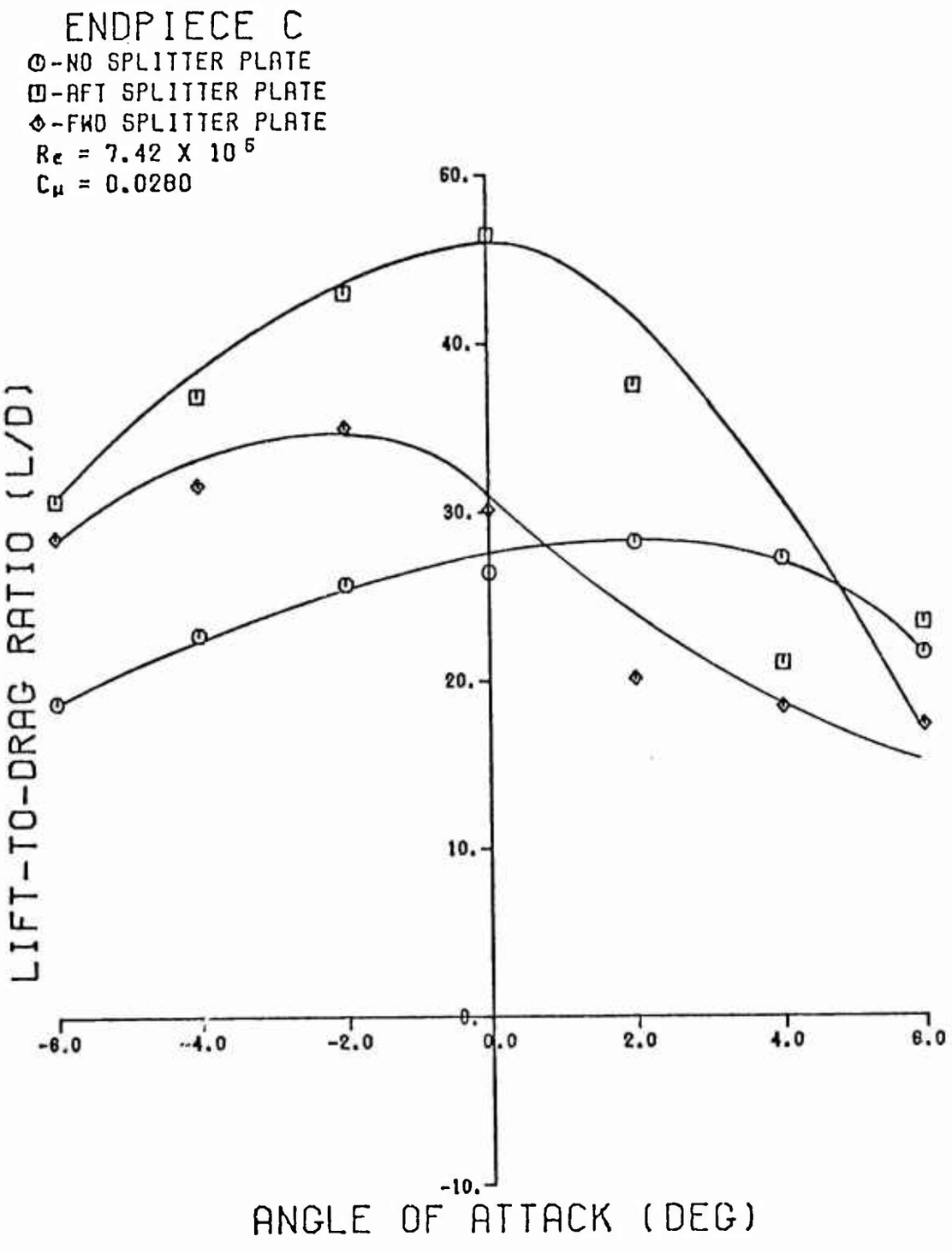

Fig. 27 The Change in L/D vs α Due to the Different Splitter Plate Configurations on Endpiece C, With Blowing

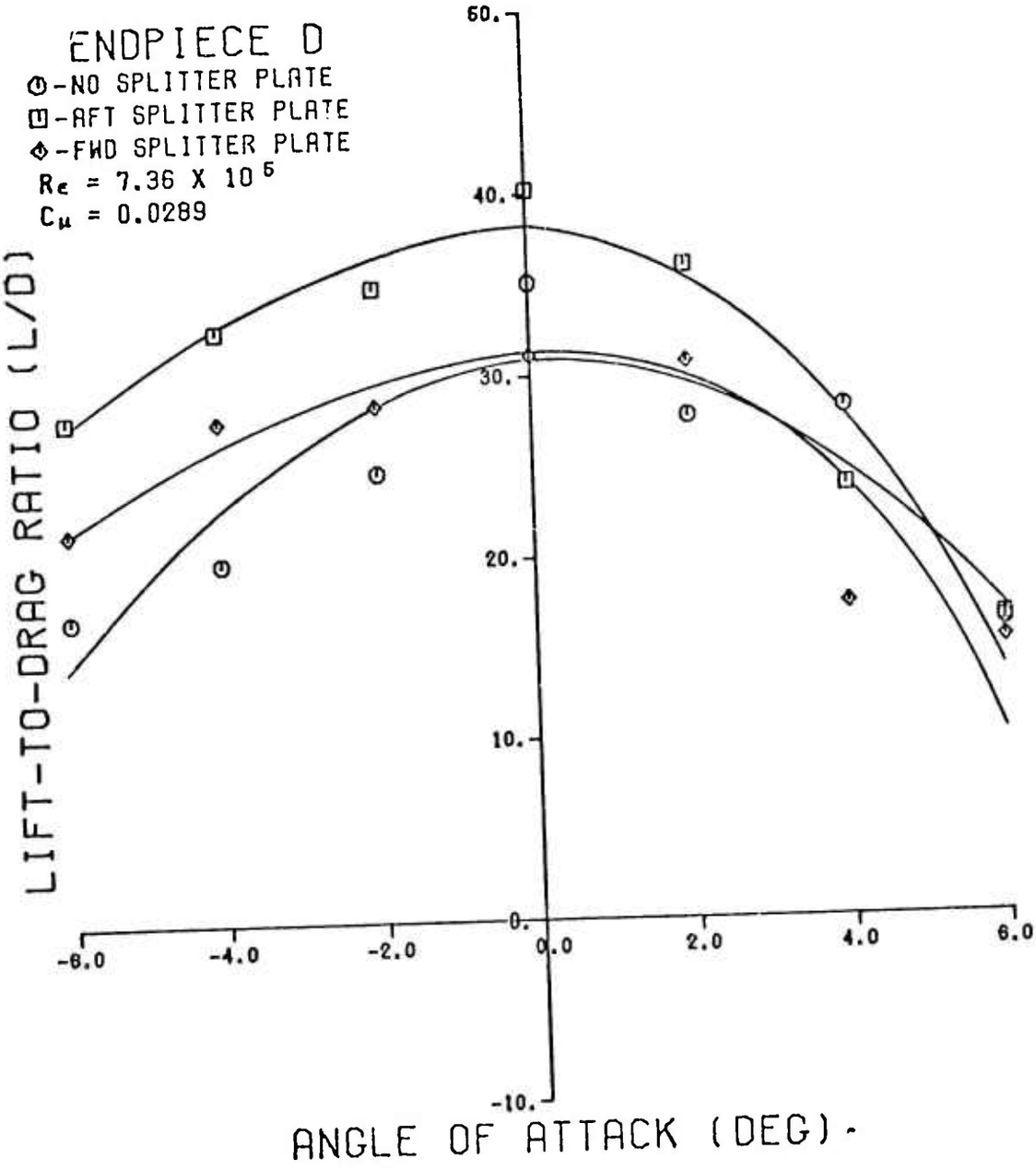

Fig. 28 The Change in L/D vs α Due to the Different Splitter Plate Configurations on Endpiece D, With Blowing

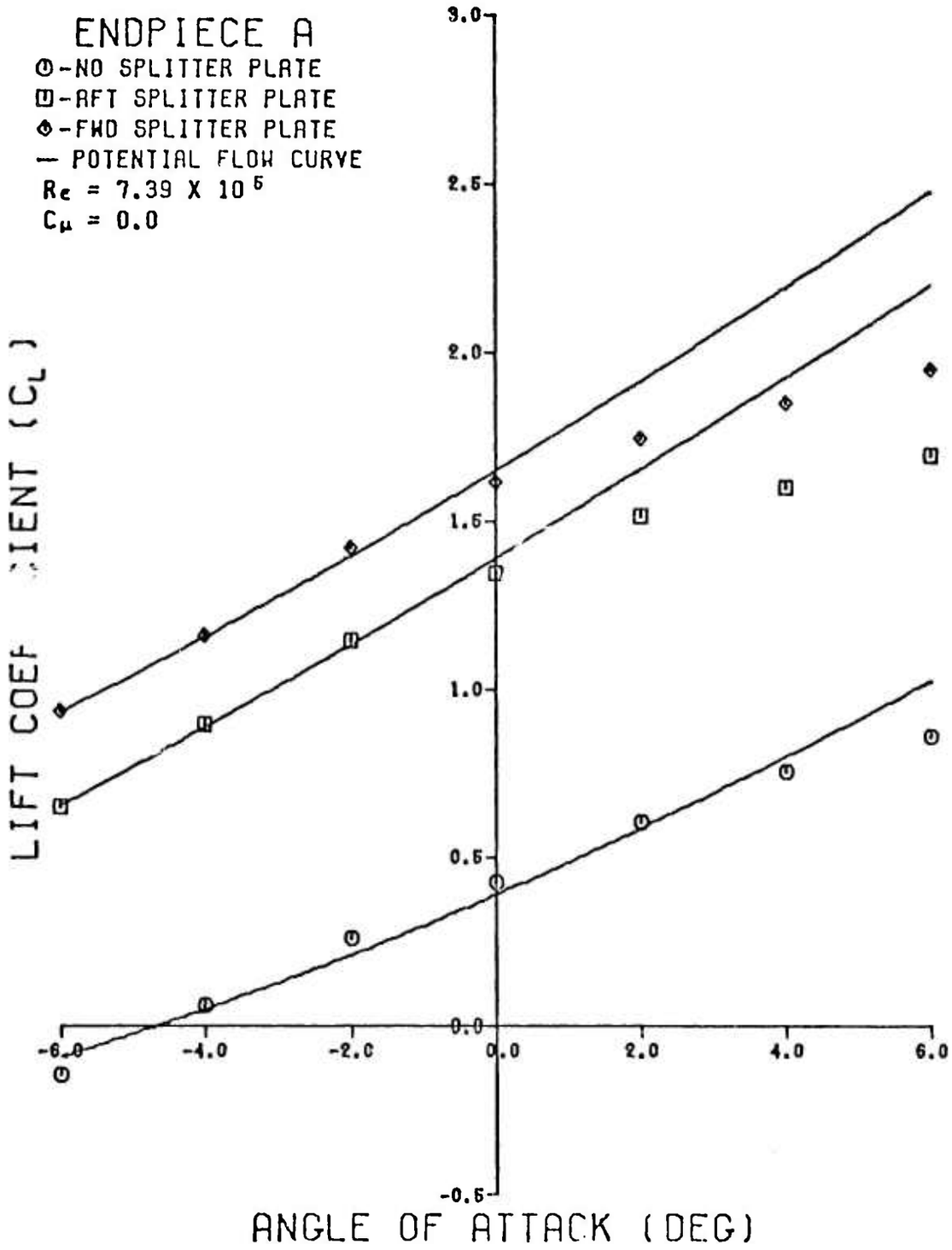

Fig. 29 The Results of Matching Potential Flow C_l's With Test C_l's on Endpiece A, Without Blowing

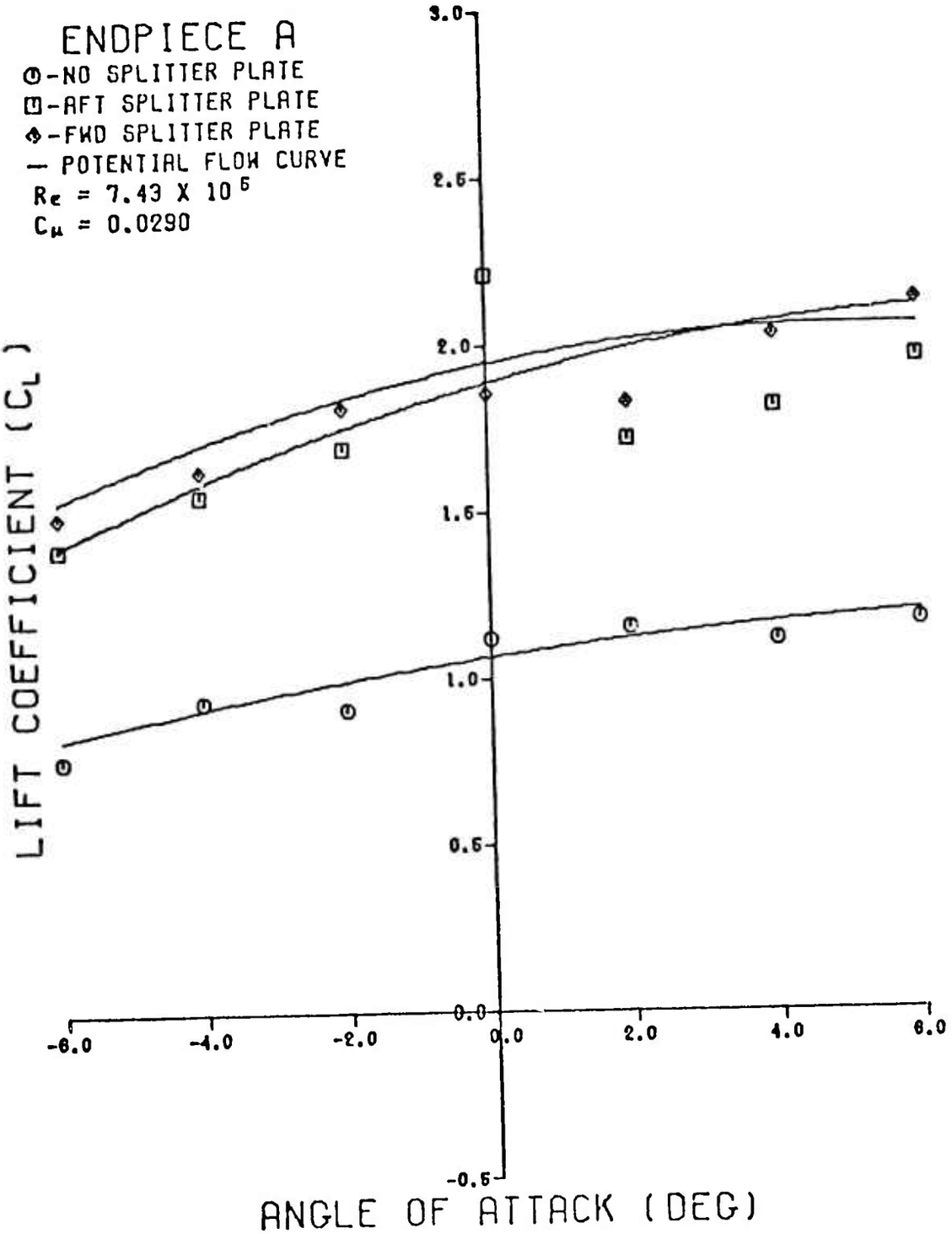

Fig. 30 The Results of Matching Potential Flow C_l's With Test C_l's on Endpiece A, With Blowing

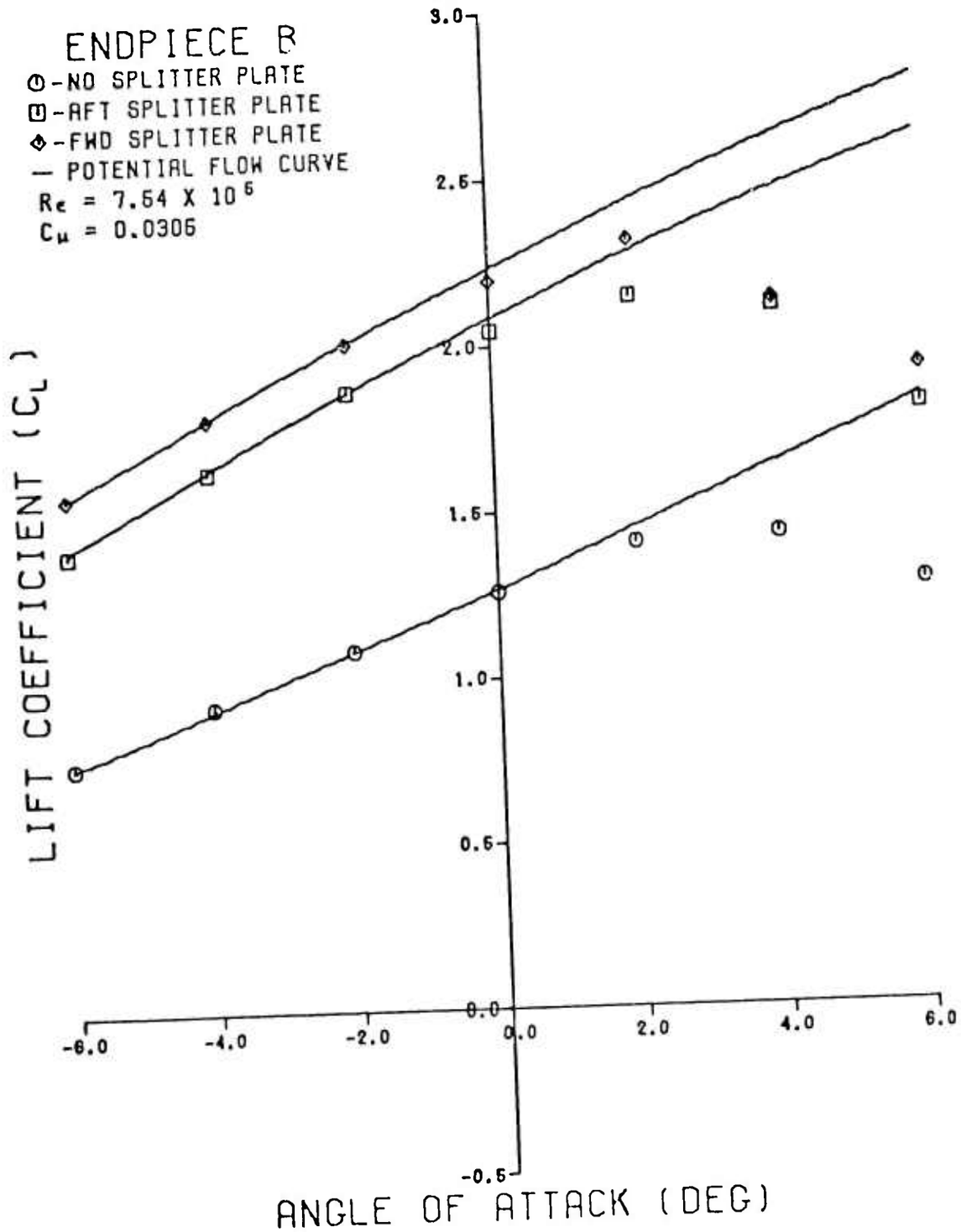

Fig. 31 The Results of Matching Potential Flow C_l's With Test C_l's on Endpiece B, With Blowing

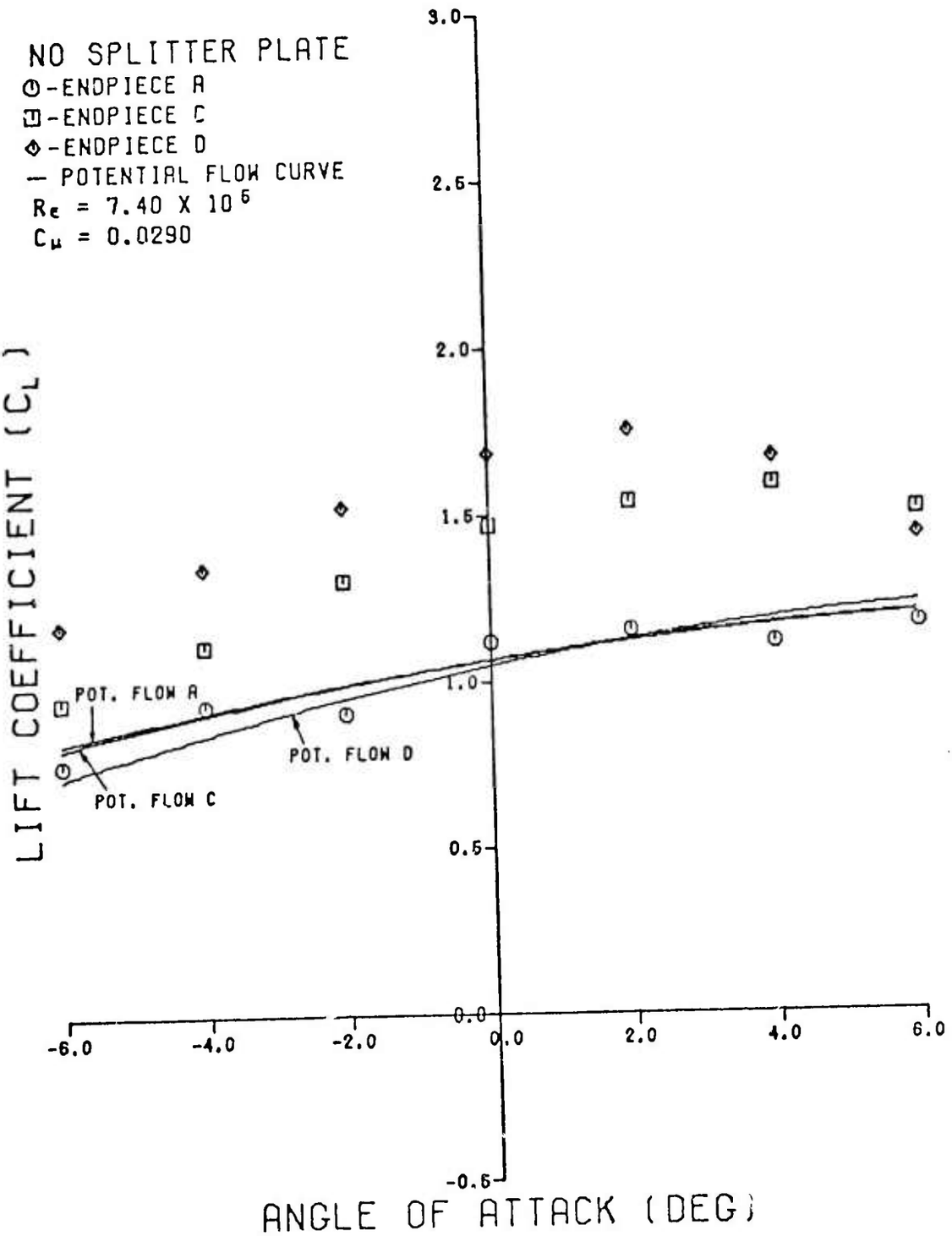

Fig. 32 A Comparison of the Results of Configuration Changes Made in the Potential Flow Program and in the Wind Tunnel Tests, With No Splitter Plate

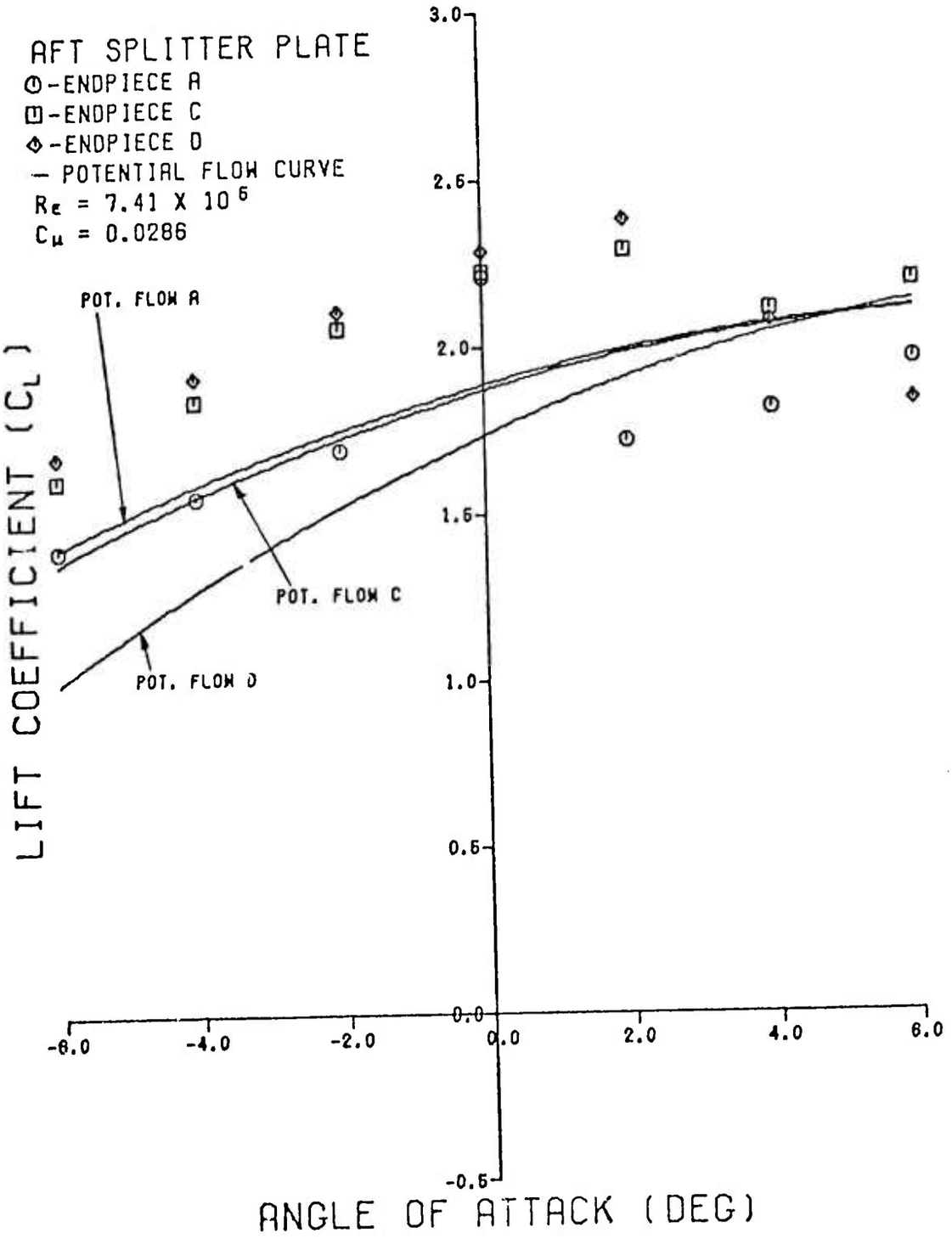

Fig. 33 A Comparison of the Results of Configuration Changes Made in the Potential Flow Program and in the Wind Tunnel Tests, With Aft Splitter Plate

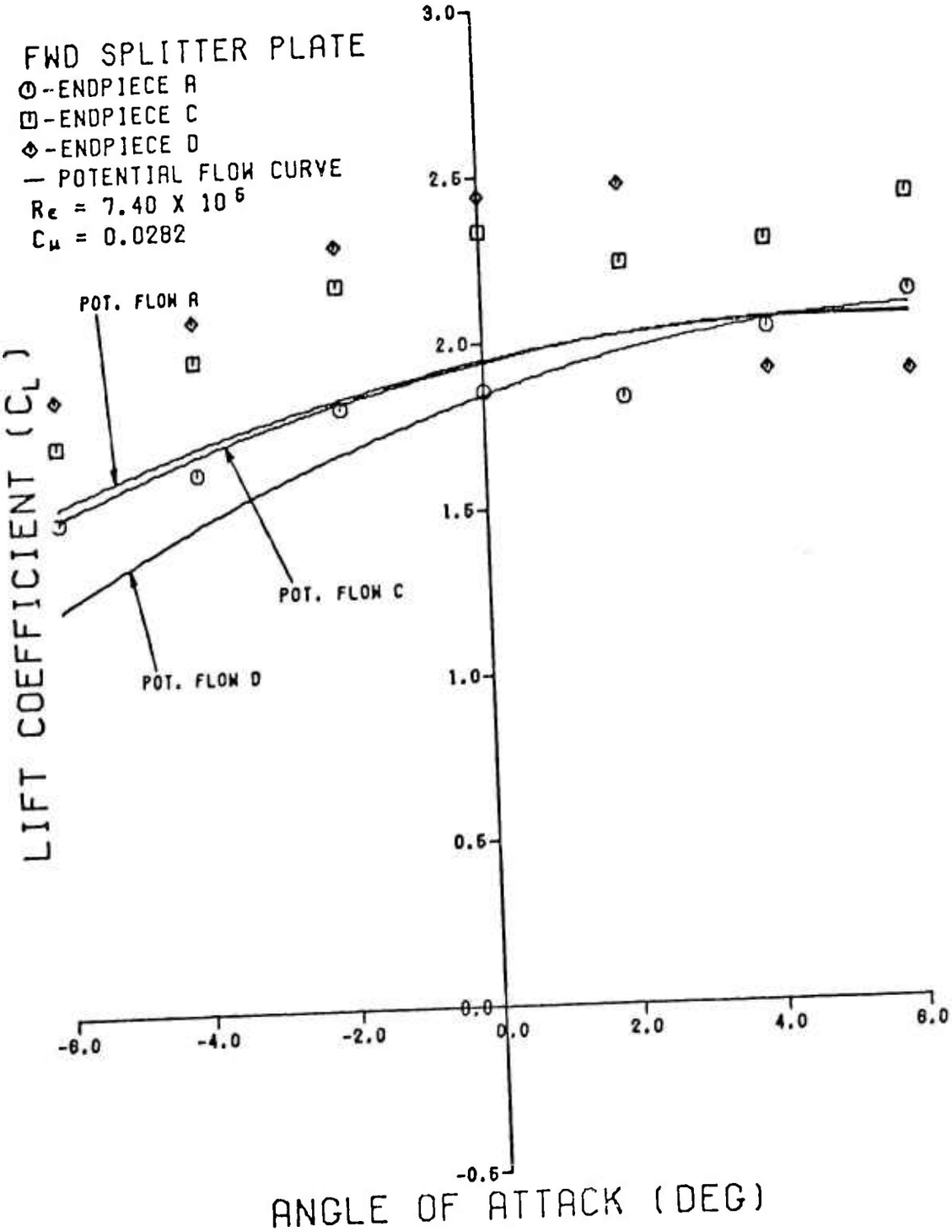

Fig. 34 A Comparison of the Results of Configuration Changes Made in the Potential Flow Program and in the Wind Tunnel Tests, With Forward Splitter Plate

Table II

The Values of the Potential Flow Program
Variable A Used to Match Lift Curve Slopes

	Angles of Attack						
	-6^o	-4^o	-2^o	0^o	2^o	4^o	6^o
Endpiece A, $C_\mu = 0.0$							
No Splitter Plate	0.85	0.60	0.35	0.10	-0.15	-0.40	-0.65
Aft Splitter Plate	-0.82	-1.00	-1.18	-1.36	-1.54	-1.72	-1.90
Forward Splitter Plate	-1.12	-1.32	-1.52	-1.72	-1.92	-2.12	-2.32
Endpiece A, $C_\mu = 0.03$							
No Splitter Plate	-0.85	-0.85	-0.85	-0.85	-0.85	-0.85	-0.85
Aft Splitter Plate	-2.40	-2.30	-2.20	-2.10	-2.00	-1.90	-1.80
Forward Splitter Plate	-2.68	-2.53	-2.38	-2.23	-2.08	-1.93	-1.78
Endpiece B, $C_\mu = 0.03$							
No Splitter Plate	-0.70	-0.85	-1.00	-1.15	-1.30	-1.45	-1.60
Aft Splitter Plate	-2.40	-2.40	-2.40	-2.40	-2.40	-2.40	-2.40
Forward Splitter Plate	-2.75	-2.75	-2.75	-2.75	-2.75	-2.75	-2.75

Vita

Richard Kirk deJonckheere was born [redacted] He graduated from [redacted] in 1970, and attended the United States Military Academy, receiving a Bachelor of Science degree and a commission in the United States Air Force in June 1974. He then entered and began study at the Air Force Institute of Technology in September 1974.

Permanent address: [redacted]

This thesis was typed by Mrs. Joyce Clark.